September 1991

MTR11277

M. M. Weiner

Performance of Ground-Based High-Frequency Receiving Arrays with Electrically-Small Ground Planes

CONTRACT SPONSOR MSR
CONTRACT NO. N/A
PROJECT NO. 91030
DEPT. D085

MITRE

The MITRE Corporation
Bedford, Massachusetts

Department Approval: _____

N. M. Tomljanovich
Department Head

MITRE Project Approval: _____

E. A. Palo
Project Leader, 91030

ABSTRACT

Electrically-small ground planes degrade the performance of ground-based high-frequency receiving arrays because the arrays are more susceptible to earth multipath, ground losses, and external currents on element feed cables. Performance degradations include a reduction in element directive gain near the horizon, distortion of the element azimuthal pattern, an increase in the system internal noise factor, and increases in the array factor root-mean-squared (rms) phase error and beam-pointing errors. The advantage of electrically-small ground planes is their relatively low cost of construction and maintenance.

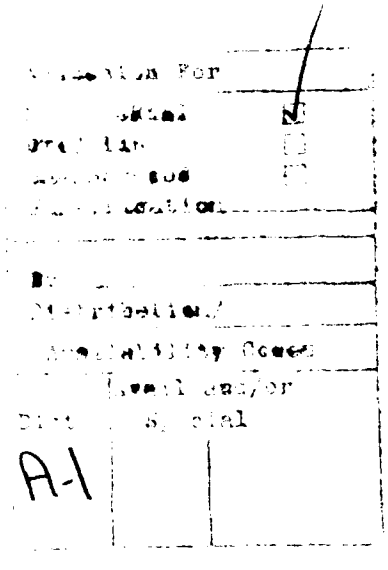

ACKNOWLEDGMENTS

Figures 2-1 through 2-13, 2-15, 3-1, 3-2, 3-3, 3-5, and 3-6 were developed under the FY90 MITRE Sponsored Research Project 91260 "High-Frequency Antenna Element Modeling," M. M. Weiner, Principal Investigator.

The computer plots of figures 3-4, 3-8, and 3-9 were developed by S. Zamoscianyk based on numerical results supplied by G. J. Burke of Lawrence Livermore National Laboratory.

TABLE OF CONTENTS

LIST OF FIGURES

LIST OF TABLES

SECTION 1

INTRODUCTION

High-frequency (HF) antenna elements for over-the-horizon (OTH) receiving arrays often consist of some form of a vertical monopole element with a ground plane resting on the Earth or in close proximity to it. Its proximity to Earth causes a far-field multipath pattern null on the horizon; multipath ground losses; a leaky evanescent surface wave which directs energy into the Earth, but not the air medium, causing additional ground losses; and a near-field non-uniform multipath reflection from a nonhomogeneous earth.

The output of each antenna element (including its matching network, if any) is usually transmitted to its own receiver by means of a transmission line (hereafter referred to as a "feed cable"). Exterior currents are induced on the element feed cables by the tangential component of the monopole element field incident on the cables and by ground-plane currents diffracted by the edge of the ground plane.

Antenna performance degradations by the Earth and by external currents on the feed cables are mitigated by employing ground planes that are as large as is economically feasible. Large ground planes bring the peak of the multipath pattern closer to the horizon, reduce near-field ground losses, provide uniform near-field ground reflection from element-to- element, shield the cables from the element fields, and minimize the ground-plane current incident on the edge of the ground plane.

In the design of very large OTH receiving arrays (comprising hundreds or thousands of elements), electrically-large metallic ground planes are prohibitively expensive to construct and maintain. One alternative approach is to employ salt-water ground planes; however, suitable salt-water sites are not readily available and they have unique problems. In this report, we discuss another alternative approach, using elements with electrically-small ground planes; and we also estimate the performance degradations that can result from it.

Performance degradations caused by electrically-small ground planes include (1) a reduction in element directive gain near the horizon (caused by Earth multipath) and distortion

of it azimuthal pattern (caused by exterior currents on element feed cables); (2) a decrease in element radiation efficiency with a consequential increase in system internal noise (caused by ground losses); (3) an increase in the array factor root-mean-squared (rms) phase error (caused by non-uniform Fresnel reflection from nonhomogeneous Earth and exterior currents on element feed cables); and (4) an increase in the array factor beam-pointing errors (caused by non-uniform Fresnel reflection from nonhomogeneous Earth).

These performance degradations may be grouped according to their effect on element directive gain, the system operating noise factor, and the array factor. The predetection signal-to-noise ratio (SNR) of a receiving system is proportional to the receive antenna directive gain (which is proportional to the element directive gain and the array factor) and is inversely proportional to the system operating noise factor [1]. For ground-based HF radar or communication systems, the Earth excess propagation loss factor is usually included in the antenna ground-plane system rather than in the propagation path [1]. Ohmic losses of the receive antenna (including its ground-plane system and matching network) are incorporated as part of the system operating noise factor [1] in accordance with International Radio Consultative Committee (CCIR) convention.

The effect of electrically-small ground planes on element directive gain is discussed in section 2. The system operating noise and array factors are discussed in sections 3 and 4, respectively. Section 5 presents the summary and conclusions.

SECTION 2

ELEMENT DIRECTIVE GAIN

Monopole elements with perfect ground planes (of infinite extent, conductivity, and density) have a radiation pattern that has its peak on the horizon and is omnidirectional in azimuth. Furthermore, the current on the exterior of the element feed cable is zero. For this case, the interference of the element and the image fields is totally constructive in the direction of the horizon, the feed cable is completely shielded from the element fields, and the current on the bottom surface of the ground plane is zero.

For imperfect ground planes, the direction of peak directive gain is at an angle above the horizon. The directive gain on the horizon is approximately -6 dBi and $-\infty$ dBi when the ground plane is in free space and when it is in proximity to flat Earth, respectively. Furthermore, the current on the exterior of the element feed cable is non-zero because the feed cable is not completely shielded from the element fields, and the current on the bottom surface of the ground plane at the feed cable is also non-zero.

This section presents numerical results of the directive gain for monopole elements with electrically-short circular ground planes resting on flat Earth. In our discussion, we assume that the element and ground planes are fabricated from metal of infinite conductivity. The ground-plane density is infinite for disk ground planes, a function of the number of radial wires and wire radius for radial-wire ground planes, and a function of the mesh spacing and wire radius for screen ground planes. The effects of Earth multipath and exterior current on the element feed cable are discussed in sections 2.1 and 2.2, respectively.

2.1 INFLUENCE OF EARTH MULTIPATH

Earth multipath introduces a null on the horizon for monopole antennas in proximity to flat Earth unless they have a perfect ground plane. In this section, we discuss the effect of Earth multipath on the element directive gain with a condition of zero exterior current on the

element feed cable. This section presents a characterization of the antenna parameters, a survey of literature, numerical results for disk ground planes and radial-wire ground planes, and an analytical expression for directive gain.

2.1.1 Characterization of Antenna Parameters

Monopole elements at the center of circular ground planes in proximity to flat Earth are characterized by at least six parameters (see figure 2-1): three antenna parameters normalized to the radio-frequency (rf) wavelength λ [element length h/λ, element radius b/λ, and ground-plane radius a/λ or $2\pi a/\lambda$ in wavenumbers]; and three Earth parameters [dielectric constant ε_r; loss tangent $(\sigma/\omega\varepsilon_0\varepsilon_r) = (60\ \lambda\ \sigma/\varepsilon_r)$; and height z_0/λ of the Earth's surface relative to the ground plane, where σ = Earth conductivity (S/m), $\omega = 2\pi f$ = radian rf frequency (rad/s), λ = rf wavelength (m), and ε_0 = free-space permittivity = 8.854×10^{-12} (farads/m)]. The Earth constants, loss tangents, and penetration depths for CCIR 527-1 characteristics of Earth in the 3 through 30 MHz band are summarized in table 2-1. The above six parameters sufficiently characterize the antenna's electrical properties for disk ground planes. For radial-wire ground planes with equally-spaced wires, additional parameters are the number N and radius b_w of the wires; for mesh-screen ground planes, the mesh shape, spacing, and wire radius are the additional parameters.

2.1.2 Survey of Literature

Numerical results of the magnetic far-field intensity with a ground plane relative to that with no ground plane (for the case of a circular ground plane resting on flat Earth) have been published previously. Wait et al. published results for small radial-wire ground planes [3]; large radial-wire ground planes [13, 17]; small disk ground planes [3]; large disk ground planes [6, 17]; large ground screens [4, 9, 12, 14]; nonhomogeneous Earth [5, 7, 8, 10, 11, 15]; and assorted ground planes [16]. Rafuse and Ruze [18] published results for large ground screens and radially-nonhomogeneous Earth. Those results yield the absolute power gain, but not the absolute directive gain, because ground losses are included in the relative magnetic far-field intensity. The above references, with the exception of 11, 12, 14, and 18, assume that the current on the finite-extent ground plane is the same as that for a perfect ground plane.

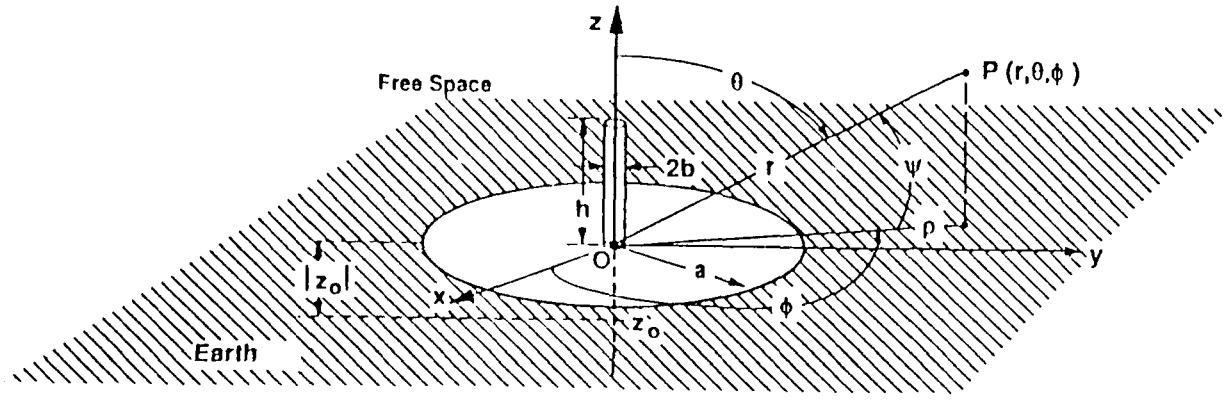

Figure 2-1. Antenna Parameters

Table 2-1. Permittivity, Loss Tangent, and Penetration Depth of CCIR 527-1 Classifications of Earth

Cases	CONSTANTS		LOSS TANGENT			PENETRATION DEPTH		
	ε_r	σ (S/m)	$\sigma/(\omega\varepsilon_r\varepsilon_0) = (60\lambda)(\sigma/\varepsilon_r)$			δ (m)		
			Frequency (MHz) [Wavelength (m)]			Frequency (MHz) [Wavelength (m)]		
			3 [99.93]	15 [19.986]	30 [9.993]	3 [99.93]	15 [19.986]	30 [9.993]
(1) Perfect Ground	1.0	∞	∞	∞	∞	0	0	0
(2) Sea Water (average Salinity 20°C)	70.0	5.0	4.282×10^{2}	8.425×10^{1}	4.283×10^{1}	1.3×10^{-1}	5.8×10^{-2}	4.1×10^{-2}
(3) Fresh Water	80.0	3.0×10^{-2}	2.251×10^{0}	4.497×10^{-1}	2.248×10^{-1}	2.1×10^{0}	1.6×10^{0}	1.6×10^{0}
(4) Wet Ground	30.0	1.0×10^{-2}	1.999×10^{0}	3.997×10^{-1}	1.999×10^{-1}	3.7×10^{0}	3.0×10^{0}	2.9×10^{0}
(5) Medium Dry Ground	15.0	1.0×10^{-3}	3.997×10^{-1}	7.995×10^{-2}	3.997×10^{-2}	2.1×10^{1}	2.1×10^{1}	2.1×10^{1}
(6) Very Dry Ground	3.0	1.0×10^{-4}	1.999×10^{-1}	3.997×10^{-2}	1.999×10^{-2}	9.2×10^{1}	9.2×10^{1}	9.2×10^{1}
(7) Pure Water, 20°C	80.0	1.8×10^{-6} 5.0×10^{-4} 1.7×10^{-3}	1.350×10^{-4} - -	- 7.495×10^{-3} -	- - 1.274×10^{-2}	2.6×10^{4} - -	- 9.4×10^{2} -	- - 2.7×10^{1}
(8) Ice (fresh water, -1°C)	3.0	6.0×10^{-5} 9.0×10^{-5} 1.0×10^{-4}	1.199×10^{-1} - -	- 3.597×10^{-2} -	- - 1.999×10^{-2}	1.5×10^{2} - -	- 1.0×10^{2} -	- - 9.2×10^{1}
(9) Ice (fresh water, -10°C)	3.0	1.8×10^{-5} 2.7×10^{-5} 3.5×10^{-5}	3.597×10^{-2} - -	- 1.079×10^{-2} -	- - 6.995×10^{-3}	5.1×10^{2} - -	- 3.4×10^{2} -	- - 2.6×10^{2}
(10) Average Land (TCI)	10.0	5.0×10^{-3}	2.998×10^{0}	5.996×10^{-1}	2.998×10^{-1}	4.8×10^{0}	1.6×10^{0}	3.4×10^{0}
(11) Free Space	1.0	0	0	0	0	∞	∞	∞

2.1.3 Numerical Results for Disk Ground Planes

Weiner [19] determined the absolute directive gain of quarter-wave monopole elements on electrically-small disk ground planes resting on flat Earth by using Richmond's method-of-moments computer programs [20, 21] which compute the actual currents on the element and ground planes and the resulting far fields. The numerical results are shown in figures 2-2 through 2-12 for the cases $h/\lambda = 0.25$, $b/\lambda = 10^{-6}$, $2\pi a/\lambda = 0$ to 8 wavenumbers, and medium dry ground ($\varepsilon_r = 15$, $\sigma = 0.001$ S/m) at a frequency of 15 MHz. Results are compared with those for a perfect ground plane ($\varepsilon_r = 1.0$, $\sigma = \infty$) and for free space ($\varepsilon_r = 1.0$, $\sigma = 0$).

The peak directivity is approximately independent of disk radius and approximately equal to that of a perfect ground plane (see figures 2-2 through 2-7). Figures 2-2 through 2-6 are polar plots of numeric directive gain on the same linear scale. The angle of incidence of the peak directivity for $0 \leq 2\pi a/\lambda \leq 8$ is approximately independent of ground-plane radius and approximately 30 degrees above the horizon (see figure 2-8). The Earth softens the edge of the ground plane and minimizes changes in directive gain resulting from ground-plane edge diffraction. In the absence of Earth, large changes in directive gain occur (see case 11 in figures 2-7 and 2-8) because ground-plane edge diffraction is more pronounced. The large changes in angle of peak directivity do not represent significant changes in peak directivity because of the broad 3 dB beamwidth of the radiation pattern. The jump in angle of peak directivity between $2\pi a/\lambda = 5.5$ and 5.75 wavenumbers (see case 11 of figure 2-8) corresponds to a change in directive gain of 0.5 dB and is due to a change in beam shape (compare figures 2-5 and 2-6). A disk radius of $2\pi a/\lambda > 60$ is required so that the angle of incidence of the peak directivity is within eight degrees of the horizon.

The directive gain at angles of incidence near the horizon ($82° \leq \theta < 90°$), for $0 \leq 2\pi a/\lambda \leq 8$, shows no improvement over that with no ground plane at all and, in fact, decreases aperiodically with increasing disk radius by as much as 1 dB (see figures 2-9 through 2-13). The directive gain at angles of incidence of 82, 84, 86, 88, and 90 degrees is 4, 5, 7, 13, and ∞ dB, respectively, below the peak directive gain for these disk radii. Substantial improvement in directive gain near the horizon occurs for $2\pi a/\lambda > 15$ as an approximate lower bound.

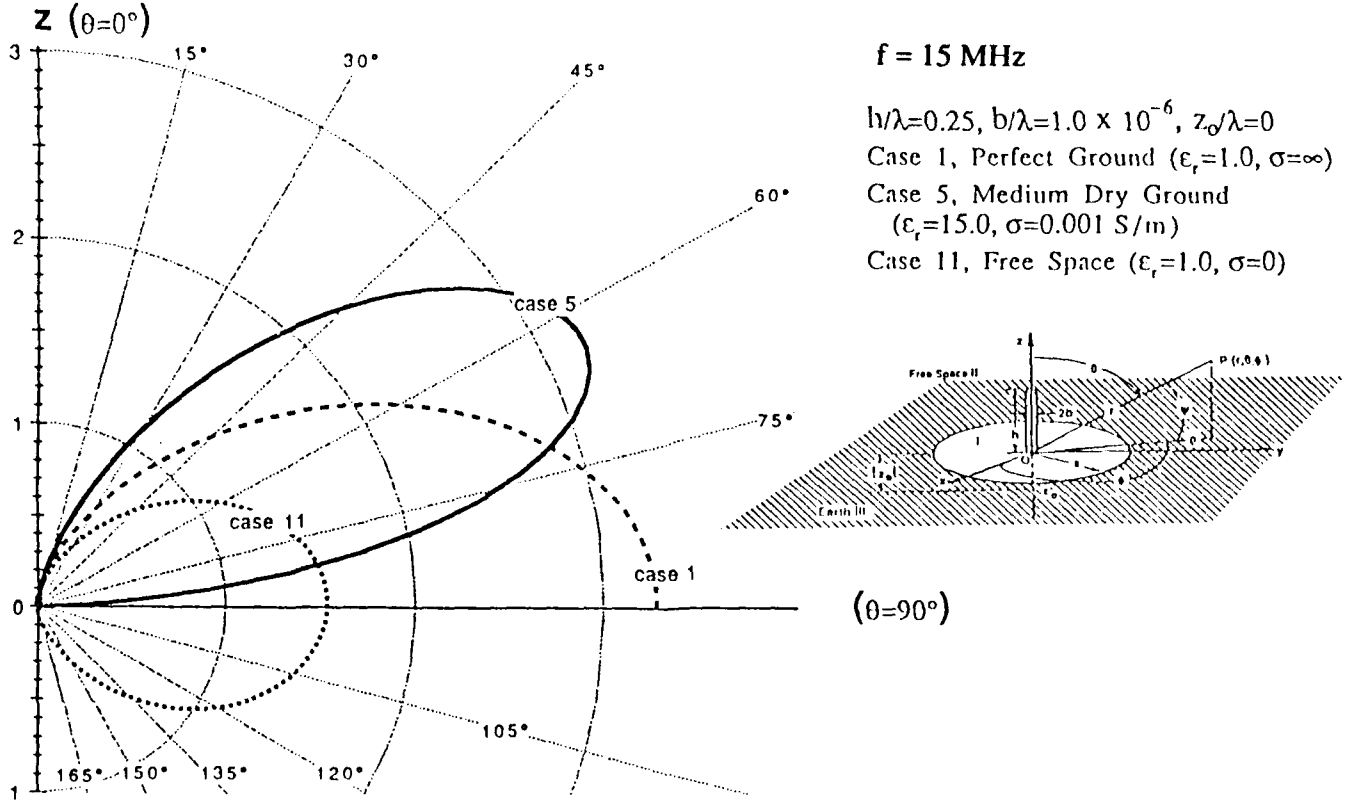

Figure 2-2. Numeric Directive Gain Polar Plot, $2\pi a/\lambda = 0.025$

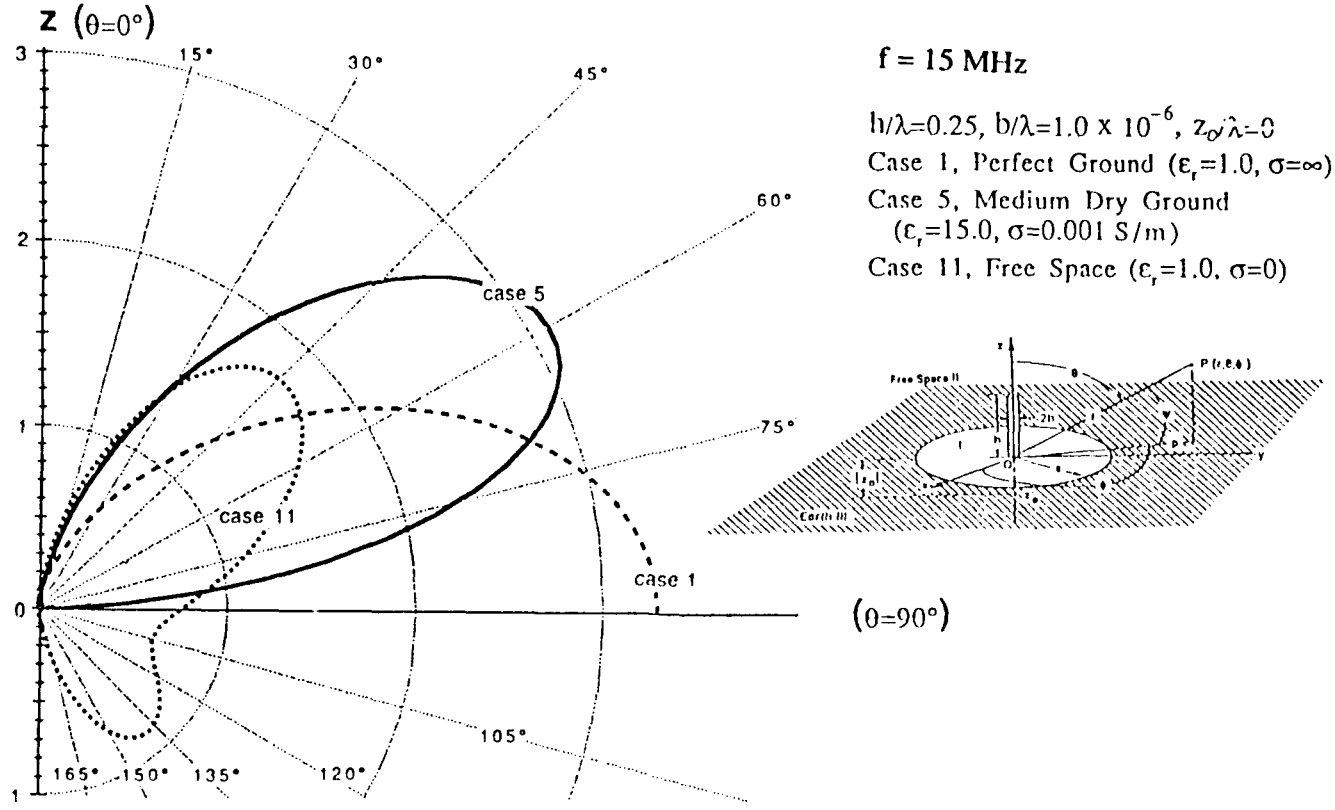

Figure 2-3. Numeric Directive Gain Polar Plot, $2\pi a/\lambda = 3.0$

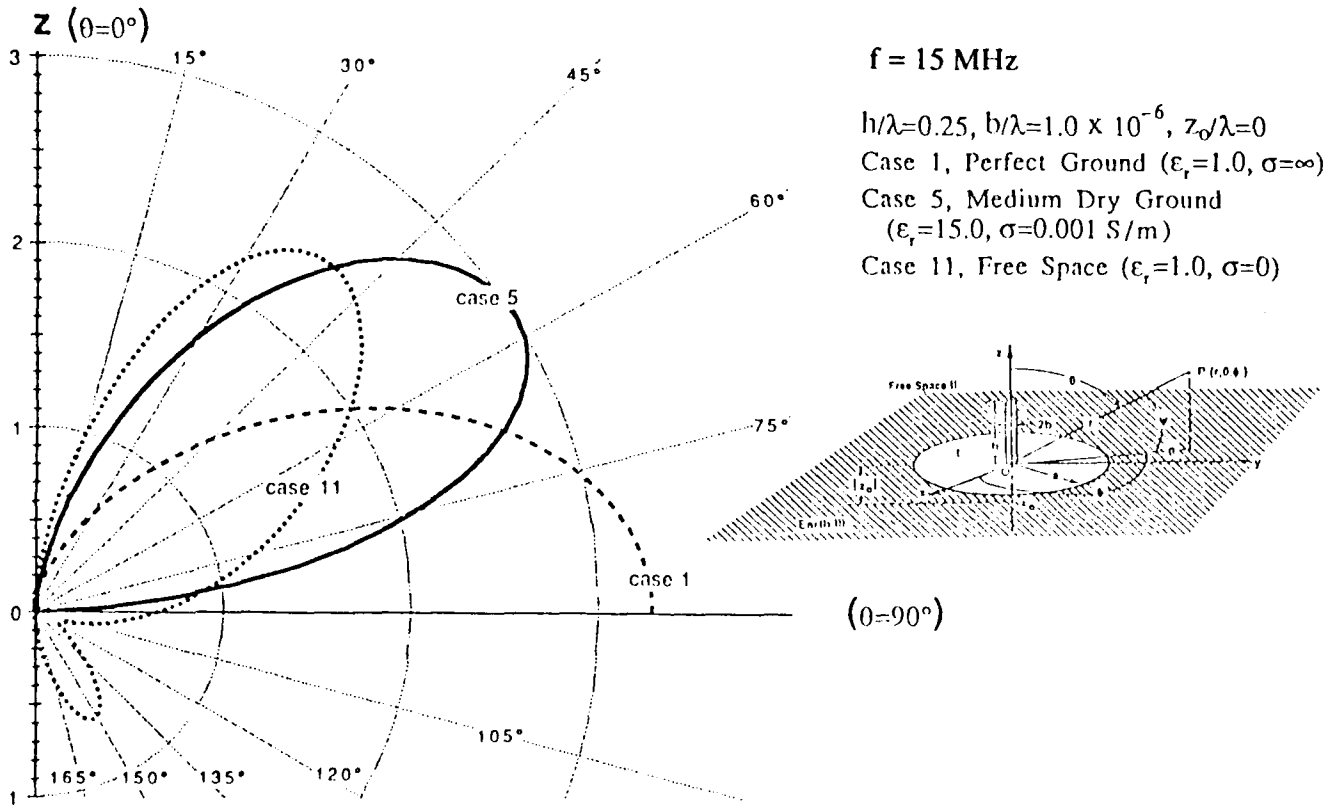

Figure 2-4. Numeric Directive Gain Polar Plot, $2\pi a/\lambda = 4.0$

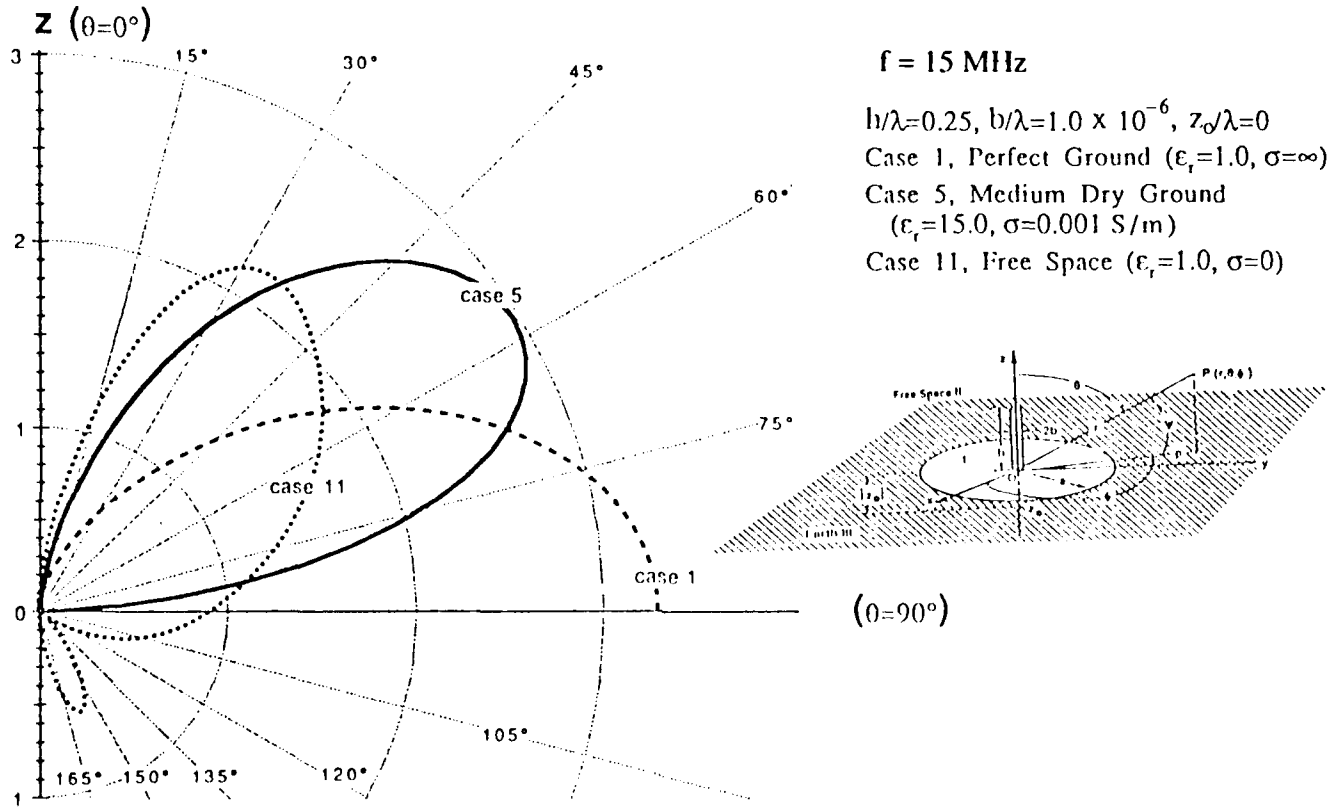

Figure 2-5. Numeric Directive Gain Polar Plot, $2\pi a/\lambda = 5.0$

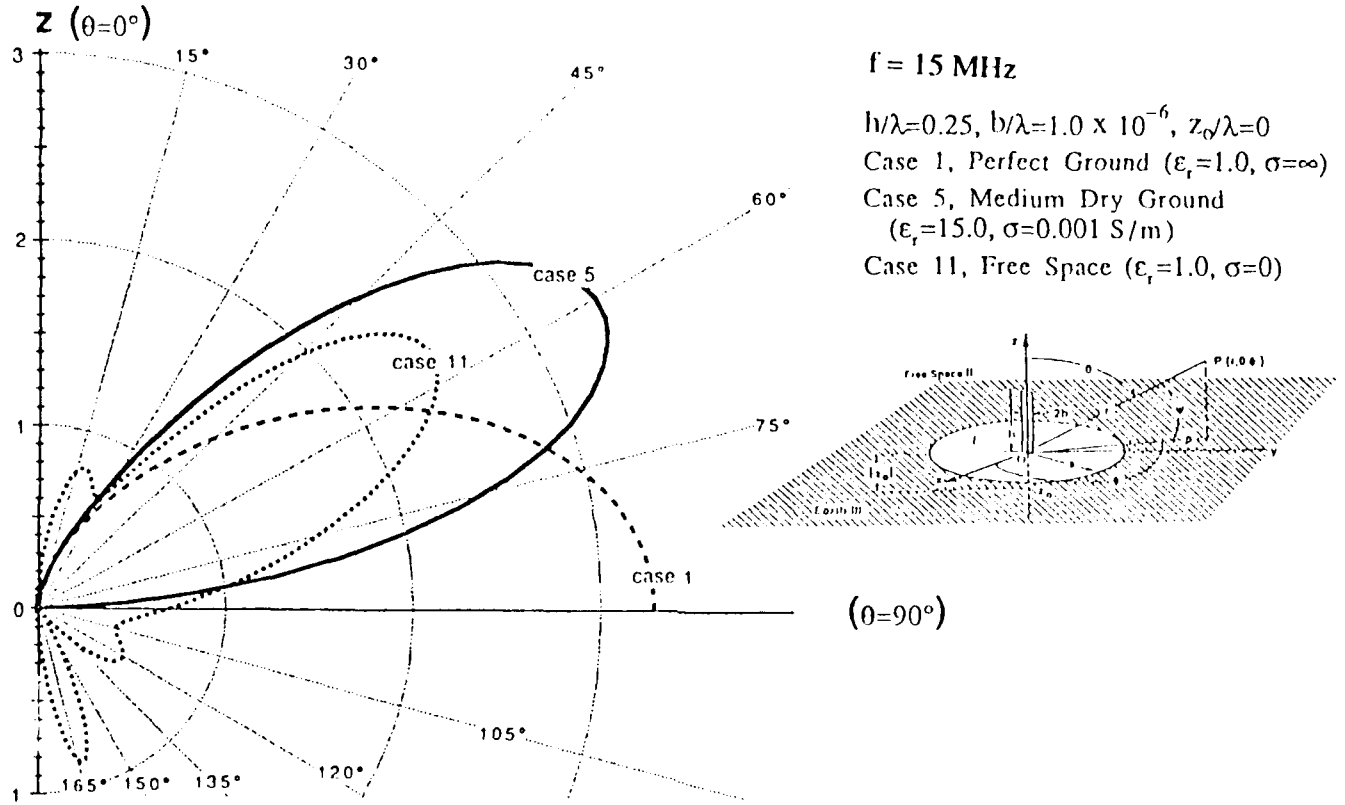

Figure 2-6. Numeric Directive Gain Polar Plot, $2\pi a/\lambda = 6.5$

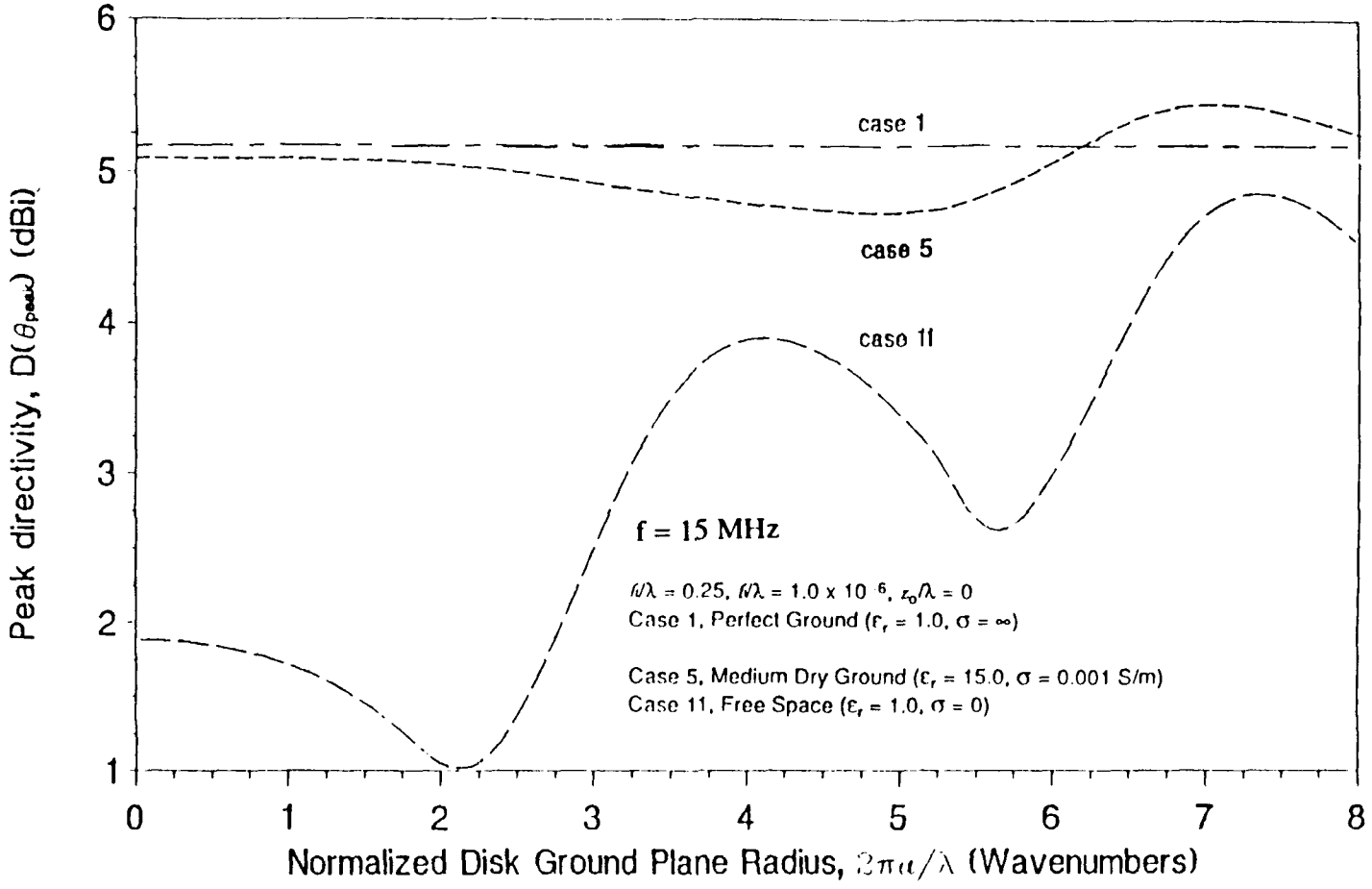

Figure 2-7. Peak Directivity

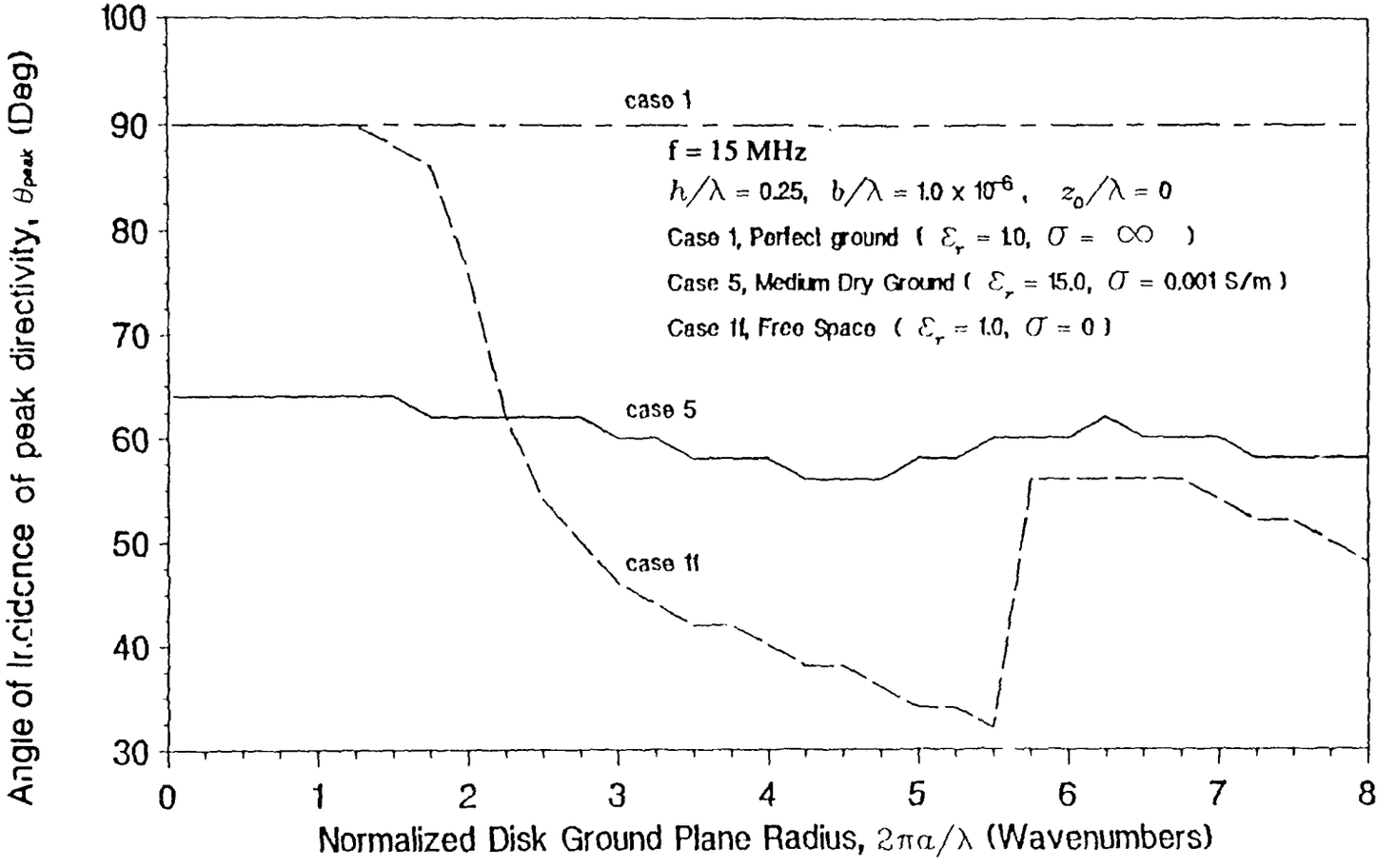

Figure 2-8. Angle of Incidence of Peak Directivity

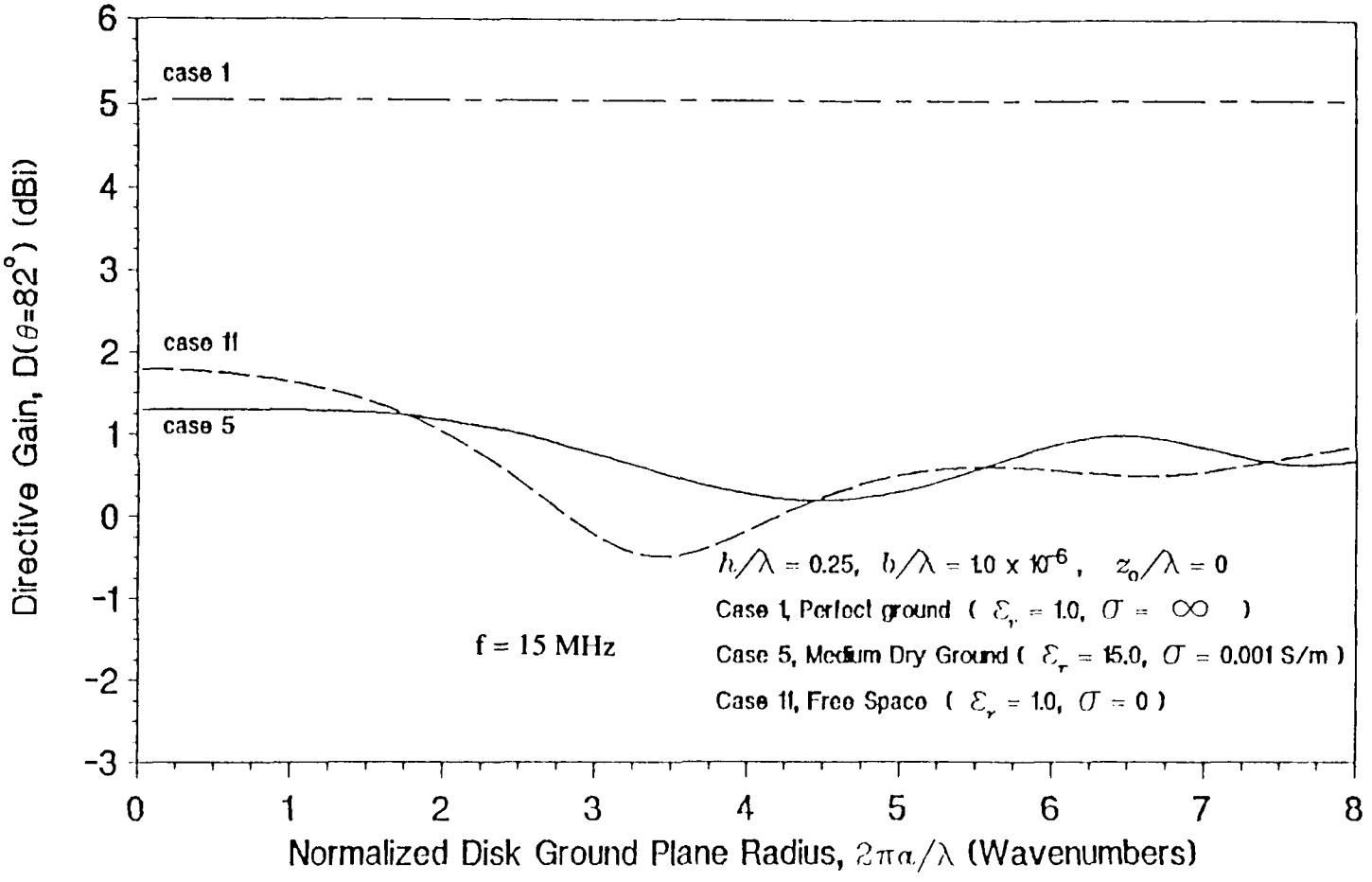

Figure 2-9. Directive Gain at Eight Degrees above the Horizon

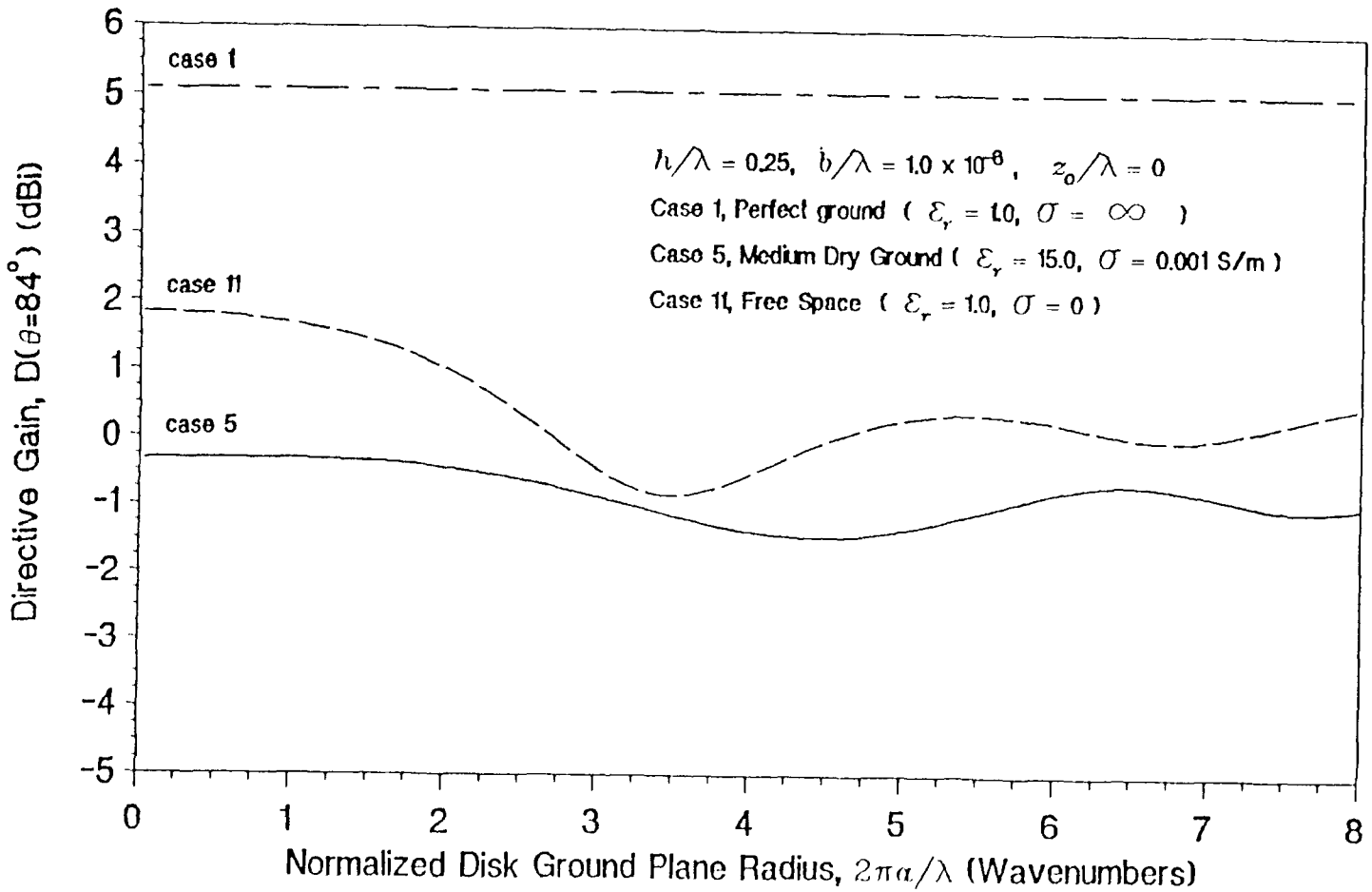

Figure 2-10. Directive Gain at Six Degrees above the Horizon

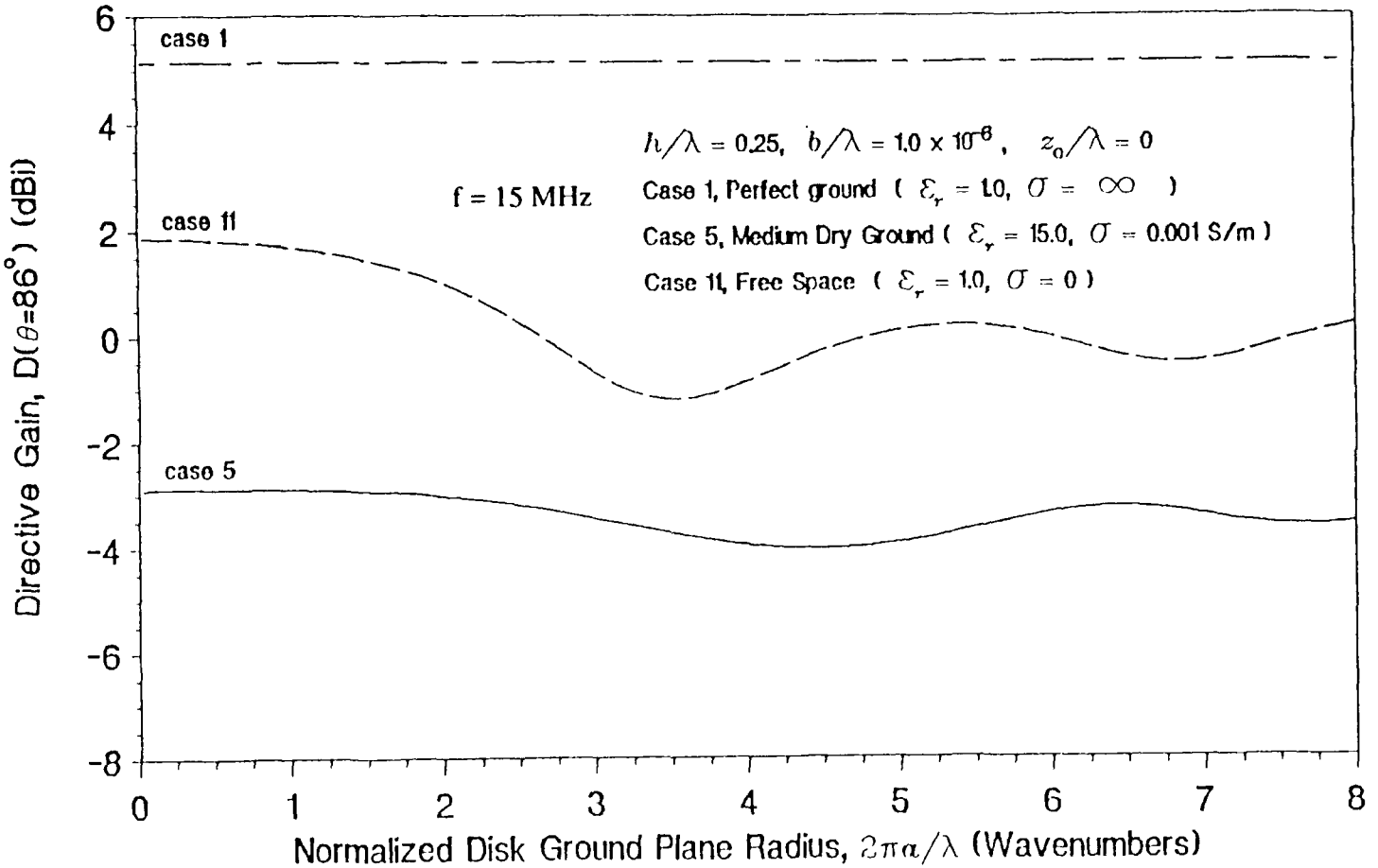

Figure 2-11. Directive Gain at Four Degrees above the Horizon

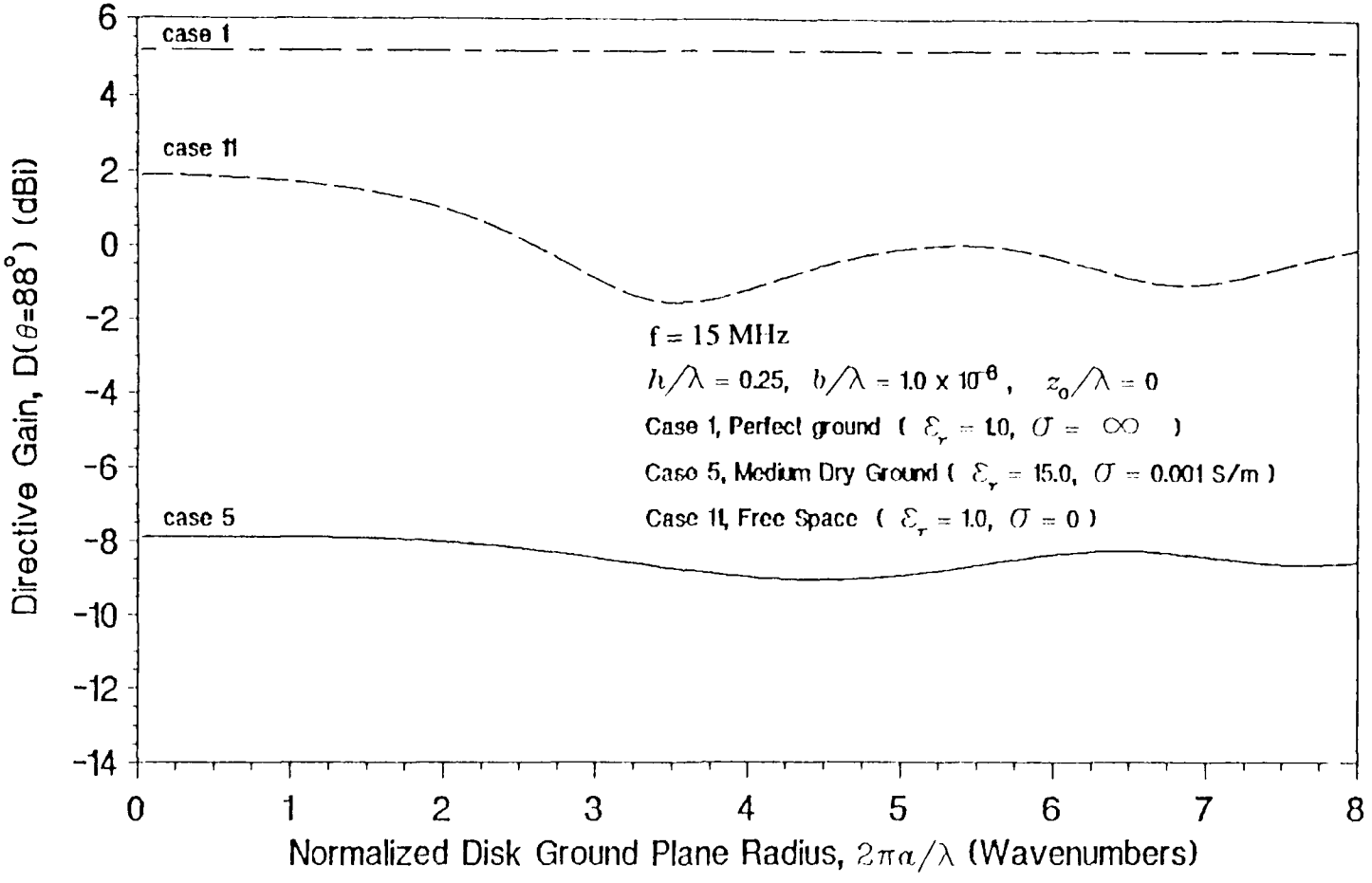

Figure 2-12. Directive Gain at Two Degrees above the Horizon

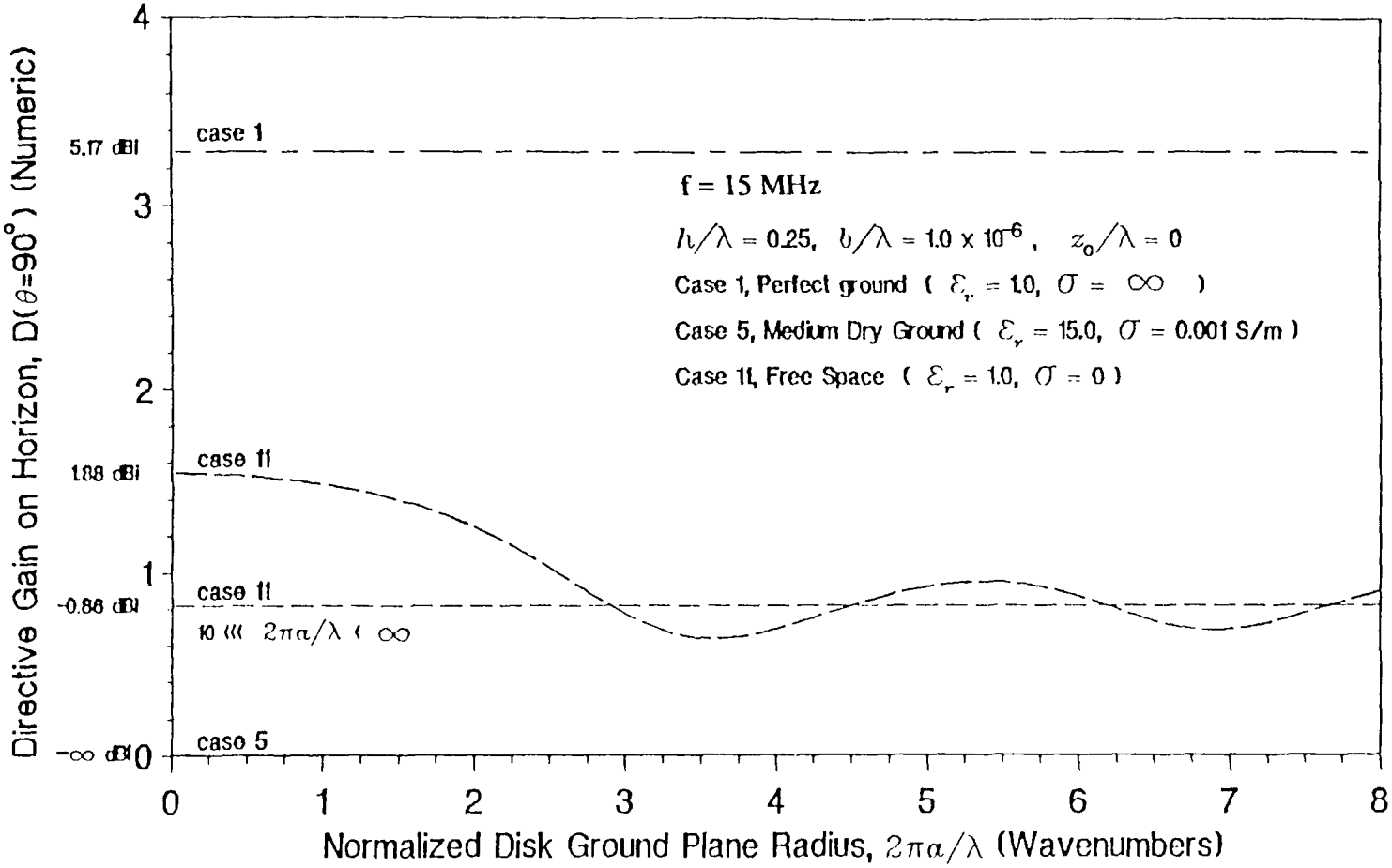

Figure 2-13. Directive Gain on the Horizon

2.1.4 Numerical Results for Radial-Wire Ground Planes

Burke, et al. [22, 23, 24, 25, 26] obtained the absolute directive gain and input impedance of quarter-wave monopole elements on electrically-small radial-wire ground planes in proximity to flat Earth, using a method-of-moments program for wire antennas known as the Numerical Electromagnetics Code (NEC). Numerical results for a test case used in Code version NEC-3 are shown in figure 2-14. The antenna parameters are $h/\lambda = 0.25$, $b/\lambda = 1.67 \times 10^{-4}$, $2\pi a/\lambda = 1.26$, $\varepsilon_r = 10.0$, $\sigma = 0.01$ S/m, N = 6, and $b_w/\lambda = 1.67 \times 10^{-4}$ at a frequency of 5 MHz. The directive gain is approximately the same as that for a disk ground plane of the same radius.

2.1.5 Analytical Expression for Directive Gain

The numeric directive gain of electrically-short monopole elements on ground planes resting on lossy Earth may be approximated analytically by an expression of the form

$$d_r(\theta) = \begin{cases} A \cos^m\theta \sin^n\theta; \ 0 \le \theta \le \pi/2 \text{ rad}, \ m > 0, \ n > 1 \\ 0, \ -\pi/2 \le \theta < 0 \text{ rad} \end{cases} \tag{2-1}$$

The exponents m and n are chosen to yield a peak directive gain in a desired direction, and a null at $\theta = 0$ and $\pi/2$ radians. The coefficient A is chosen to satisfy the condition

$$(1/4\pi) \int_0^{2\pi} \int_0^{\pi/2} d_r(\theta) \sin\theta \, d\theta \, d\phi = 1$$

Accordingly,

$$A = 2 / \int_0^{\pi/2} \cos^m\theta \sin^{n+1}\theta \, d\theta$$

IL2671

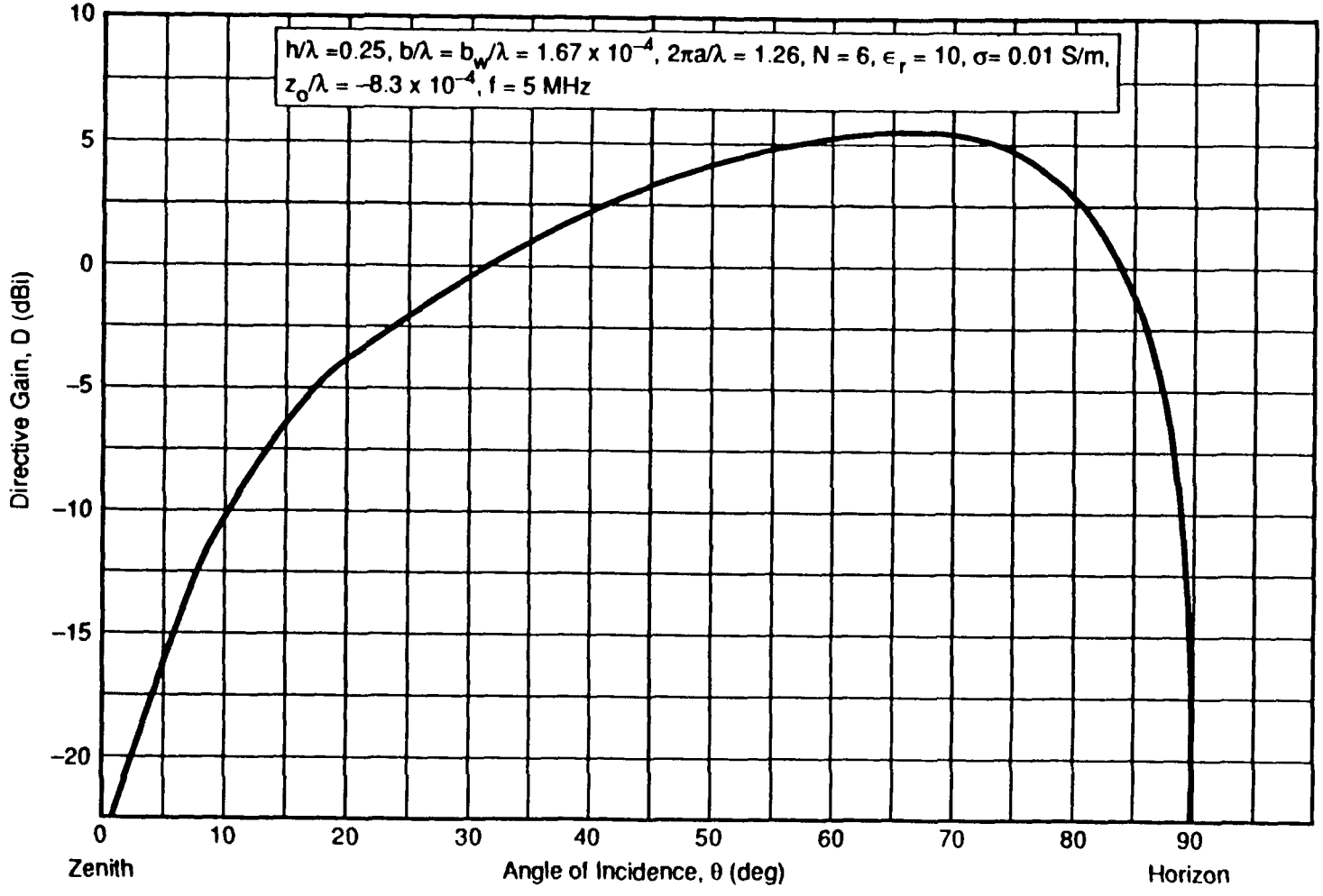

Figure 2-14. Directive Gain of Radial-Wire Ground Plane, $2\pi a/\lambda = 1.26$

The directive gain of equation (2-1) has a null in the direction of zenith, and the horizon has a peak directive gain comparable to that for a perfect ground plane.

An analytical expression that approximates the directive gain obtained by numerical methods for medium dry ground and $2\pi a/\lambda = 3$ (see figure 2-15) is given by

$$d_r(\theta) = \begin{cases} 10\cos\theta \sin^3\theta; 0 \le \theta \le \pi/2 \text{ rad} \\ 0, -\pi/2 \le \theta < 0 \text{ rad} \end{cases} \quad (2\text{-}3)$$

Equation (2-3) has a peak directive gain $d_{r\,peak} = 3.25 = 5.12$ dBi in the direction $\theta = \pi/3$ radians. The directive gain of electrically-short monopole elements on ground planes resting on lossy Earth does not vary appreciably with different types of lossy Earth or for ground-plane radii $0 \le 2\pi a/\lambda \le 8$ wavenumbers. Therefore, equation (2-3) is also an approximation of the directive gain obtained by numerical methods for cases (3) through (10) of table 2-1 and ground-plane radii $0 \le 2\pi a/\lambda \le 8$ wavenumbers. A more accurate analytical expression of the directive gain for a specific case is obtained by optimizing the exponents m and n in equation (2-1), and modifying the coefficient A in accordance with equation (2-2).

2.2 DEGRADATION BY FEED-CABLE EXTERIOR CURRENT

The condition of zero exterior current on the feed cable is never realized for monopole elements with imperfect ground planes. However, this condition is approximated in practice with lossy ferrite toroidal cases around the feed cable [2]. The ferrite toroids must extend along the cable to a distance so that the element field impinging upon the cable is sufficiently weak and the current (edge-diffracted underneath the ground plane to the feed cable) is adequately attenuated.

The exterior current on the feed cable may also be minimized by burying the cable below the surface of the Earth at a sufficient depth. The depth can be much less than the field penetration depth. For example, the penetration depth for a plane-wave incident normally on

IL2838

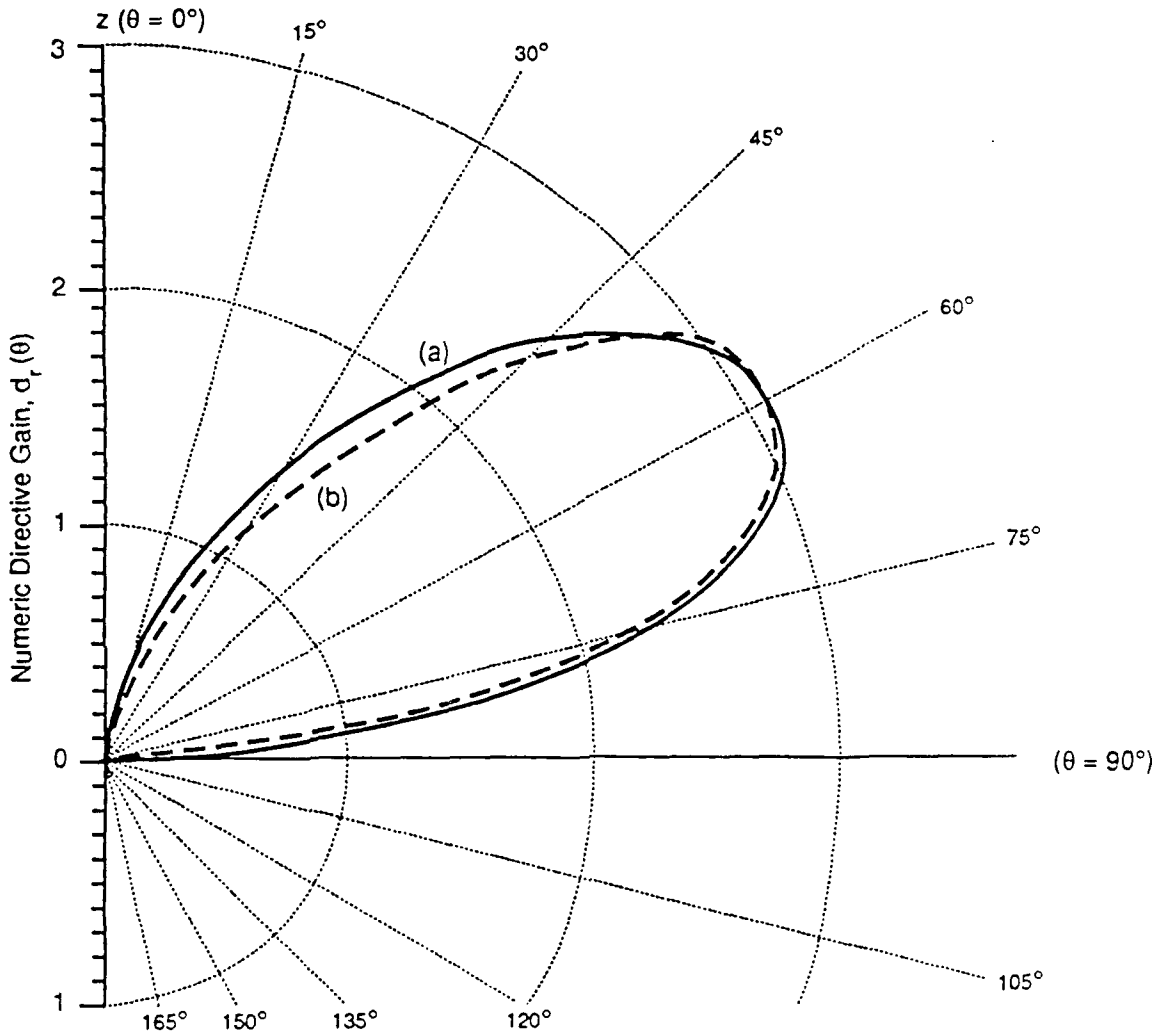

$h/\lambda = 0.25$, $b/\lambda = 1.0 \times 10^{-6}$, $z_o/\lambda = 0$, f = 15 MHz
Case 5, Medium Dry Ground
($\varepsilon_r = 15.0$, $\sigma = 0.001$ S/m)

Figure 2-15. Numeric Directive Gain of a Quarter-Wave Element on a Disk Ground Plane Resting on Medium Dry Ground, $2\pi a/\lambda = 3.0$ (a) Richmond's Method-of-Moments; (b) $10 \cos \theta \sin^3 \theta$

medium dry ground at 15 MHz is 21m (see table 2-1). If the feed cable is buried at a depth of 21cm (1/100 of the penetration depth), most of the exterior current that is generated on the feed cable will not be reradiated into the air medium; instead, it will be leaked off into the Earth.

A more detailed discussion of performance degradation by feed-cable exterior current is forthcoming [49].

SECTION 3

SYSTEM OPERATING NOISE FACTOR

The predetection SNR of a receiving system is inversely proportional to the system operating noise factor f [1]. If the ambient temperatures of the receiving antenna, matching network, and transmission line are equal to the reference temperature, then

$$f = (f_a - 1 + \ell_c\, \ell_m\, \ell_n\, f_r)\, f_p \tag{3-1}$$

where

f_a = receive antenna external noise factor integrated over the antenna pattern function (numeric)

ℓ_c, ℓ_m, ℓ_n = available loss factors of the receive antenna, matching network, and transmission line, respectively (numeric ≥ 1)

f_r = receiver noise factor (numeric)

f_p = signal-to-noise processing factor (numeric)

For an external noise-limited system, the system operating noise factor given by equation (3-1) reduces to

$$f \approx f_a f_p \quad , \quad f_a >> \ell_c\, \ell_m\, \ell_n\, f_r - 1 \tag{3-2}$$

where $\ell_c\ \ell_m, \ell_n, f_r$ are internal noise parameters generated by the receiving system. When the receiving system is externally noise-limited, which is one of the design objectives of the HF receiving system, the system operating noise factor is minimized and the predetection SNR is maximized. This condition is expressed as

$\ell_c \ell_m \ell_n f_r - 1 << f_a$, externally noise-limited receiving system.

The external noise factor f_a is a function of the directive gain of the receive antenna [1]. The available loss factors ℓ_c, ℓ_m, ℓ_n and the receiver noise factor f_r are evaluated in references 1, 28, and 29 as functions of the circuit impedance parameters and source impedances of the respective circuits. The available loss factors are equal to the ratio of the input to output available powers of the respective circuits, which is unity when the ohmic loss of the circuit is zero. The ohmic loss of the receive antenna earth-ground system is conventionally included in the available loss factor ℓ_c of the receive antenna (rather than in the excess propagation loss factor) in HF receive systems [1]. The receiver noise factor f_r is a function of the receiver source admittance and four empirical noise parameters of the receiver [28].

The parameters $f_a, \ell_c, \ell_m, \ell_n, f_r$ are all functions of the extent, conductivity, and density of the receive antenna ground plane. The parameters ℓ_m, ℓ_n , and f_r, which are indirect functions of these ground-plane parameters, become stabilized (as a function of ground-plane radius and Earth permittivity) for small ground planes (see section 3.2). The antenna available loss factor ℓ_c, a direct monotonic function of these ground-plane parameters, requires a much larger ground plane before becoming stabilized (see section 3.1).

3.1 INFLUENCE OF GROUND LOSSES ON THE ANTENNA AVAILABLE LOSS FACTOR

The antenna available loss factor ℓ_c is defined as the ratio of the available power at the input of the antenna to the radiated far-field power. For an antenna in free space or in proximity to dielectric Earth ($\sigma = 0$), the far-field power is radiated into the hemispheres above and below the antenna. However, for an antenna in proximity to lossy Earth ($\sigma > 0$), the radiated far-field power is confined to the hemisphere above the Earth because any power radiated downward into lossy Earth is attenuated at large distances at a rate greater than $1/r^2$. The antenna available loss factor ℓ_c is given in reference 28 as:

$$\ell_c = 1/\eta = R_{in}/R_{rad} = 1 + (R_c/R_{rad}) \qquad (3\text{-}3)$$

where

η = antenna radiation efficiency = fraction of the available input power that is radiated to the far field (numeric ≥ 1)

R_{in} = antenna input resistance = $R_c + R_{rad}$ (ohms)

R_{rad} = antenna radiation resistance (ohms)

R_c = series resistance due to ohmic losses of the antenna circuit including ground losses, but excluding losses in the matching network (ohms)

The series resistance R_c is only from ohmic losses in the Earth because the element and ground plane are assumed to be fabricated from metal of infinite conductivity.

Hansen [30] has determined the radiation efficiency η of vertical elements with electrically-small ground planes in proximity to lossy Earth ($\sigma > 0$) for Hertzian and half-wave dipoles above lossy Earth. Weiner [19] has determined the radiation efficiency for quarter-wave monopole elements on disk ground planes resting on Earth, and Burke [33] has determined it for quarter-wave elements on radial-wire ground planes in proximity to Earth.

In addition to the radiation efficiency η, we define a modified radiation efficiency η_d that is equal to the ratio of the far-field power radiated in the hemisphere above the Earth to the available input power. Their relationship, for the cases of an element above lossy Earth ($\sigma > 0$) or in free space ($\varepsilon_r = 1$, $\sigma = 0$), is given by:

$$\eta_d = \begin{cases} \eta, \text{ element above lossy Earth } (\sigma > 0) \text{ or a perfect ground plane } (\sigma = \infty) \\ \eta/2, \text{ element in free space } (\varepsilon_r = 1, \sigma = 0) \\ P_{air}/(P_{air} + P_{earth}), \text{ element above dielectric Earth } (\sigma = 0) \end{cases} \qquad (3\text{-}4)$$

where

P_{air} = far-field power radiated into upper hemisphere (air)
P_{earth} = far-field power radiated into lower hemisphere (earth)

For an element above dielectric Earth ($\sigma = 0$), the antenna radiation efficiency is $\eta = 1$ since the element and ground plane have been assumed to be fabricated from metal of infinite conductivity. King [31] and Burke [32] have determined the modified radiation efficiency η_d for a Hertzian dipole above dielectric Earth.

The following subsections present numerical results of Earth-ground losses for these cases: a vertically-polarized dipole above lossy Earth, a vertically-polarized Hertzian dipole above dielectric Earth, a quarter-wave monopole element on a disk ground plane resting on Earth, and a quarter-wave monopole element on a radial-wire groundscreen in proximity to Earth. A discussion of the role of the surface wave in directing energy into the Earth is included.

3.1.1 Vertically-Polarized Dipole above Lossy Earth

The radiation efficiency of a vertical dipole above lossy Earth increases non-monotonically with increasing height above Earth; monotonically with increasing length of the dipole; and non-monotonically with increasing conductivity of the Earth [30]. Minimum radiation efficiency occurs for a Hertzian dipole at zero height above the Earth. Its numerical value is not clear in reference 30. For lossy earth ($\sigma > 0$), computer runs of the NEC-3 program using the Sommerfeld option yield a minimum radiation efficiency $\eta = 0$ *in the limit of the dipole length h approaching zero and the dipole height* $|z_o|$ approaching zero (see table 3-1). A Fresnel reflection coefficient model is grossly inaccurate in computing absolute power gain, ground losses, radiation efficiency, or input impedance for an element above lossy Earth (see table 3-1 for an electrically-small monopole element whose base rests on Earth), although such a model accurately computes the absolute directive gain [51]. A Fresnel reflection coefficient model yields results for directive gain similar to those obtained by Richmond's method-of-moments for

IL2740

Table 3-1. Radiation Efficiency of a Vertically-Polarized Thin Monopole Element of Length h Whose Base Is at Zero Height above Earth, f = 15 MHz

CCIR-527-1 Earth Classification	Radiation Efficiency η (numeric)					
	h/λ = 0.01	h/λ = 0.05	h/λ = 0.10	h/λ = 0.15	h/λ = 0.20	h/λ = 0.25
(1) Perfect Ground						
Sommerfeld	1.000	1.000	1.000	1.000	1.000	1.000
Fresnel	1.000	1.000	1.000	1.000	1.000	1.000
(2) Sea Water						
Sommerfeld*	0.005	0.317	0.660	0.752	0.798	0.823
Fresnel	0.894	0.891	0.889	0.886	0.882	0.877
(3) Fresh Water						
Sommerfeld*	0.000	0.014	0.083	0.146	0.211	0.273
Fresnel	0.525	0.520	0.517	0.511	0.504	0.496
(4) Wet Ground						
Sommerfeld*	0.000	0.005	0.033	0.063	0.101	0.144
Fresnel	0.407	0.402	0.399	0.393	0.387	0.379
(5) Medium Dry Ground						
Sommerfeld*	0.000	0.008	0.050	0.087	0.125	0.163
Fresnel	0.318	0.316	0.315	0.313	0.309	0.305
(6) Very Dry Ground						
Sommerfeld*	0.000	0.003	0.020	0.039	0.063	0.090
Fresnel	0.175	0.175	0.175	0.175	0.176	0.178
(7) Pure Water, 20 °C						
Sommerfeld*	0.002	0.096	0.216	0.282	0.334	0.375
Fresnel	0.510	0.510	0.508	0.505	0.501	0.495
(8) Ice, –1 °C						
Sommerfeld*	0.000	0.003	0.020	0.039	0.063	0.090
Fresnel	0.175	0.175	0.175	0.176	0.176	0.178
(9) Ice, –10 °C						
Sommerfeld*	0.000	0.008	0.046	0.077	0.107	0.135
Fresnel	0.175	0.175	0.175	0.176	0.177	0.179
(10) Average Land (TCI)						
Sommerfeld*	0.000	0.001	0.007	0.016	0.027	0.044
Fresnel	0.294	0.287	0.282	0.277	0.270	0.262
(11) Free Space						
Sommerfeld	1.000	1.000	1.000	1.000	1.000	1.000
Fresnel	1.000	1.000	1.000	1.000	1.000	1.000

* More accurate result

Sommerfeld ≡ NEC-3 program in Sommerfeld option with voltage excitation source between earth and the base of the element ($b/\lambda = 10^{-5}$)

Fresnel ≡ Program MODIFIED IMAGES assuming Fresnel reflection coefficient and sinusoidal current distribution on elements

disk ground planes when the disk radius approaches zero, but it yields different results from Richmond's method-of-moments for input impedance, absolute power gain, and radiation efficiency. The Fresnel reflection coefficient model accurately calculates the relative energy reflected in various directions into the upper hemisphere, but it neglects the leaky evanescent surface wave that is generated by the incident spherical wavefront in proximity to the air-earth interface (see section 3.1.5).

3.1.2 Vertically-Polarized Hertzian Dipole above Dielectric Earth

For a vertically-polarized Hertzian dipole at zero height ($| z_0 | \rightarrow 0$) above dielectric Earth, the modified radiation efficiency η_d is greater than zero for $\varepsilon_r < \infty$ and is equal to 0.09 - 0.10 for $9 \leq \varepsilon_r \leq 81$ (see figures 3-1 and 3-2 showing data generated by King [31] and Burke [32]). King's results, based on a Sommerfeld integral model, are approximate because his analytical formulation is subject to the condition $\varepsilon_r >> 1$ (or equivalently, $k_1/k_2 \geq 3$). However, Burke's results, which are based on the NEC-3 method-of-moment's program, are considered to be the best available.

The absolute directive gain pattern of a vertically-polarized Hertzian dipole at zero height above dielectric Earth is shown in figure 3-3 for the case $\varepsilon_r = 9$. It was generated by using the Sommerfeld option of the NEC-3 program with a voltage excitation source between the base of an electrically-short ($h/\lambda = 2 \times 10^{-4}$), electrically-thin ($b/\lambda = 2 \times 10^{-4}$), monopole element and dielectric Earth. In the upper hemisphere (air), the radiation pattern is similar to that for the case of lossy Earth, except that the peak directive gain is reduced by approximately 11 dB (compare with figures 2-2 and 2-7). In the lower hemisphere (dielectric Earth), however, the radiation pattern is remarkable because most of the energy is radiated at the critical angle θ_c. The peak directive gain is 15.6 dBi at an angle of transmission $\theta_t = 19.5$ degrees, which in reference 33 is shown to correspond to

$$\theta_t = \theta_c = \arcsin [(\varepsilon_r)^{-1/2}], \text{ Hertzian dipole on dielectric Earth} \qquad (3\text{-}5)$$

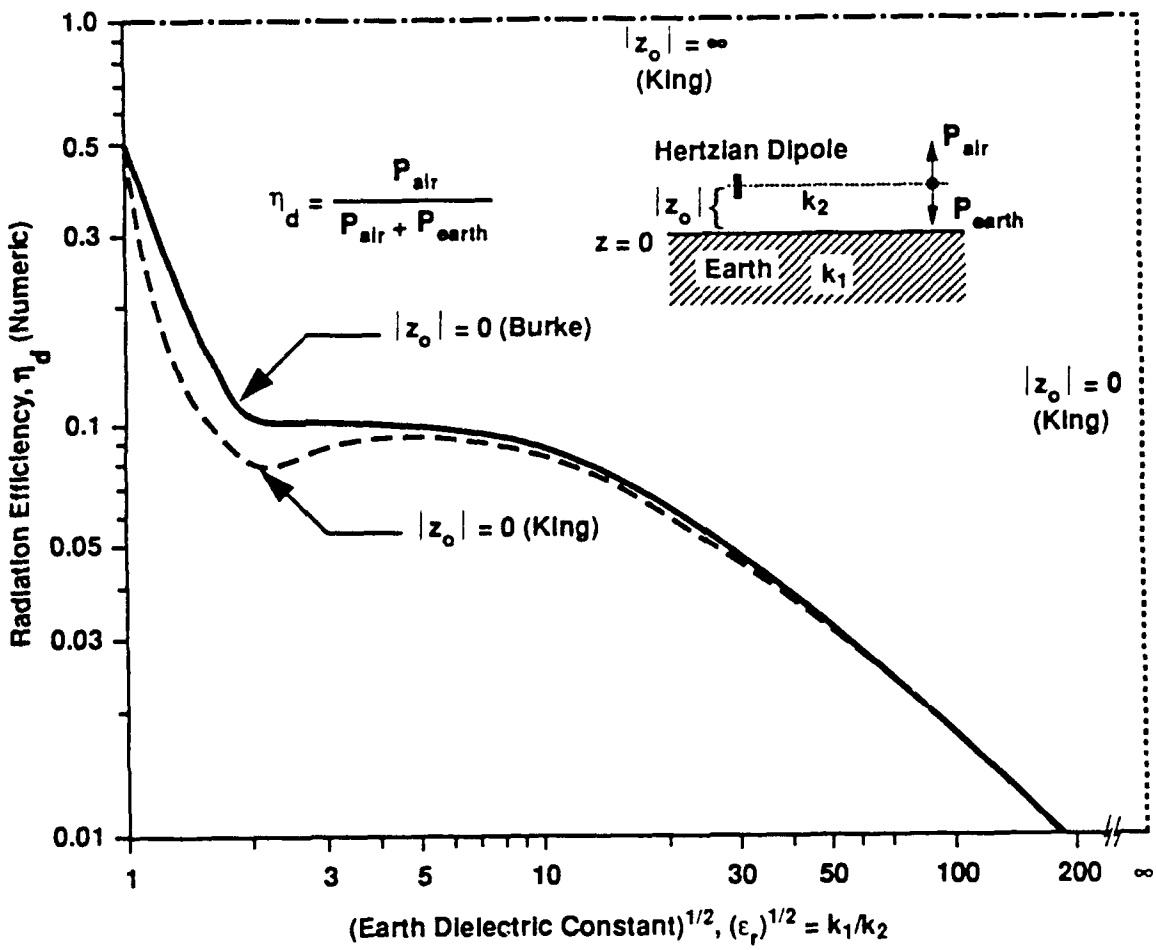

Figure 3-1. Radiation Efficiency of Vertically-Polarized Hertzian Dipole above Dielectric Earth, $|z_0|/\lambda = 0$ and $|z_0|/\lambda = \infty$

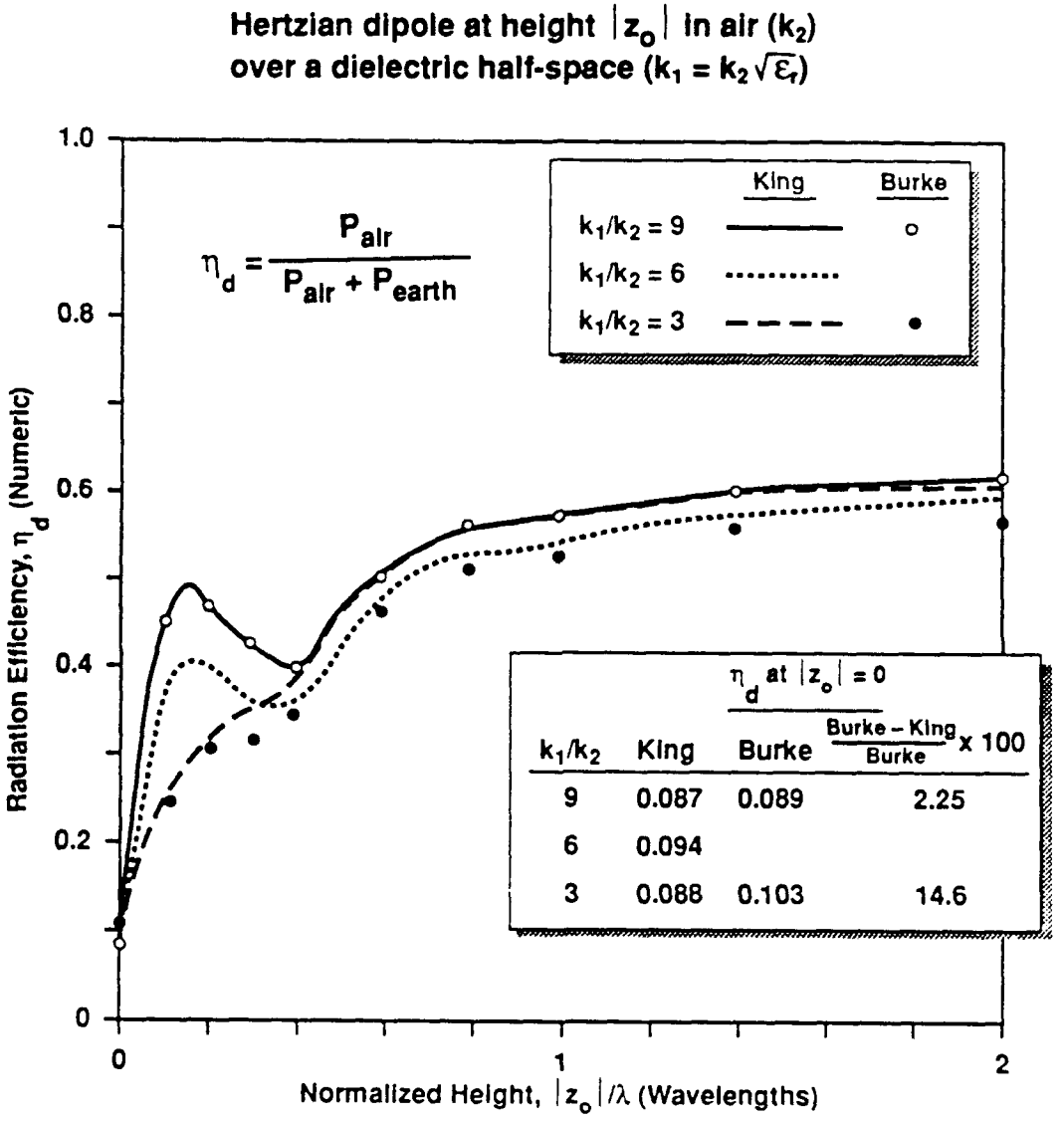

Figure 3-2. Radiation Efficiency of Vertically-Polarized Hertzian Dipole above Dielectric Earth, $0 \leq |z_o|/\lambda \leq 2$

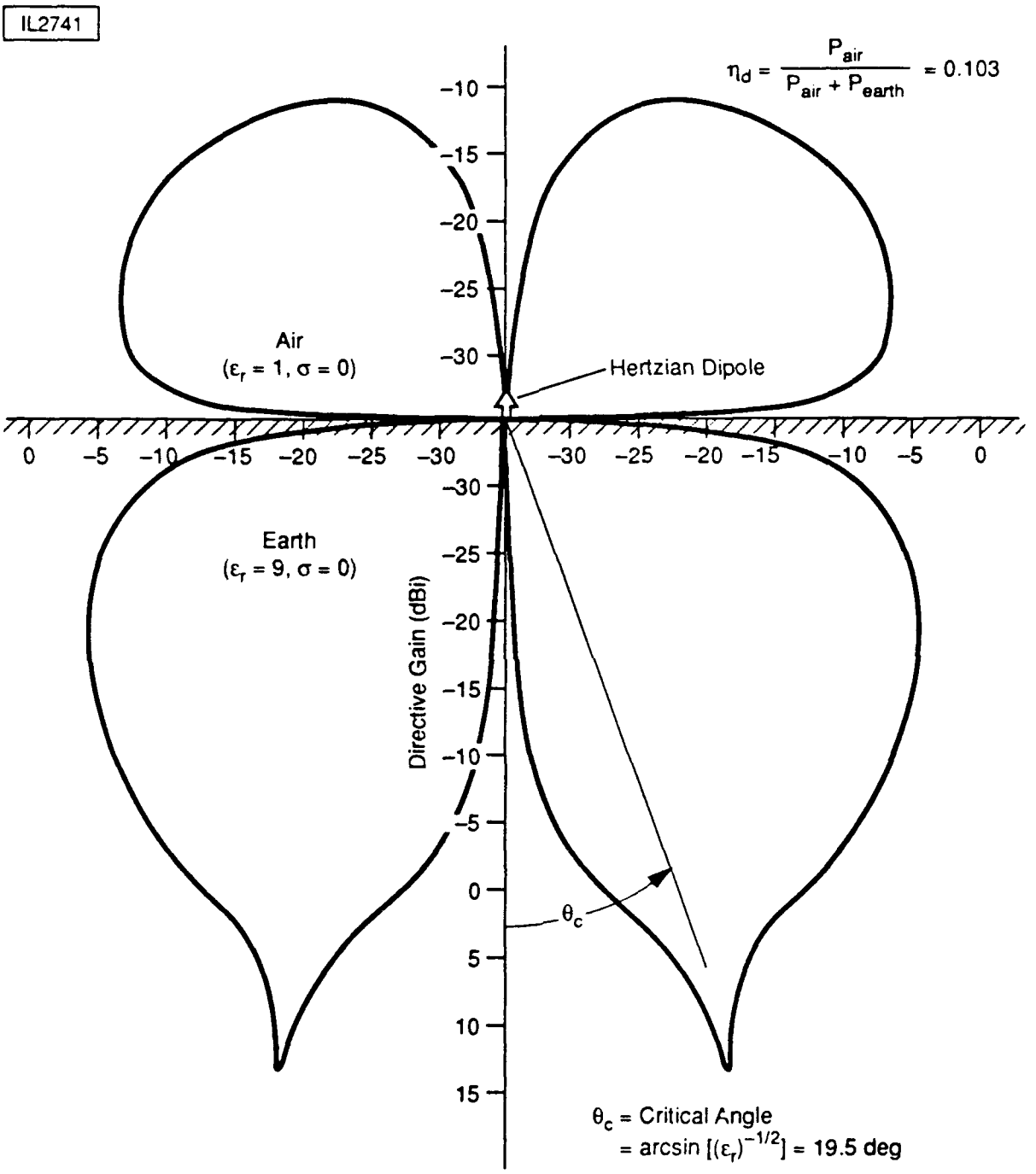

Figure 3-3. Directive Gain (in any Azimuthal Plane) of a Vertically-Polarized Hertzian Dipole at Zero Height Above Dielectric Earth, $\varepsilon_r = 9$

where

θ_c = critical angle = angle of reflection for a plane-wave incident from a less dense medium at an angle of incidence approaching $\pi/2$ radians.

The modified radiation efficiency is $\eta_d = 0.103$ (see figure 3-3). The fraction of the available input power that is transmitted into the dielectric Earth is $1 - \eta_d = 0.897$ (compare with 1.0 for lossy Earth), which is transmitted to the far field (compare with zero for lossy Earth) at the critical angle θ_c. The role of the surface wave in directing energy into the earth is discussed in section 3.1.5.

3.1.3 Quarter-Wave Monopole Element on a Disk Ground Plane Resting on Earth

Weiner [19] has used Richmond's method-of-moments [20, 21] to obtain the radiation efficiency of quarter-wave monopole elements on disk ground planes resting on Earth for the CCIR-527-1 classifications given in table 2-1. The radiation efficiency η increases monotonically with increasing disk radius a (see figure 3-4).

3.1.4 Quarter-Wave Monopole Element on a Radial-Wire Groundscreen in Proximity to Earth

Numerical results for the radiation efficiency of quarter-wave monopole elements with radial-wire groundscreens in proximity to Earth have been obtained by Burke [33] and Weiner [50] using Burke's method-of-moments code NEC-GS. These results are plotted in figure 3-5 for the groundscreen buried at a depth of $z_o/\lambda = 10^{-4}$ in Earth of relative complex permittivity $\varepsilon^*/\varepsilon_o = 15 - j1.5$. This permittivity corresponds approximately to medium dry ground at a frequency of 15 MHz (see case 5 of table 2-1). The radiation efficiency increases monotonically with increasing length and number of radial wires (see figure 3-4) and the length of the monopole element (as deduced from table 3-1).

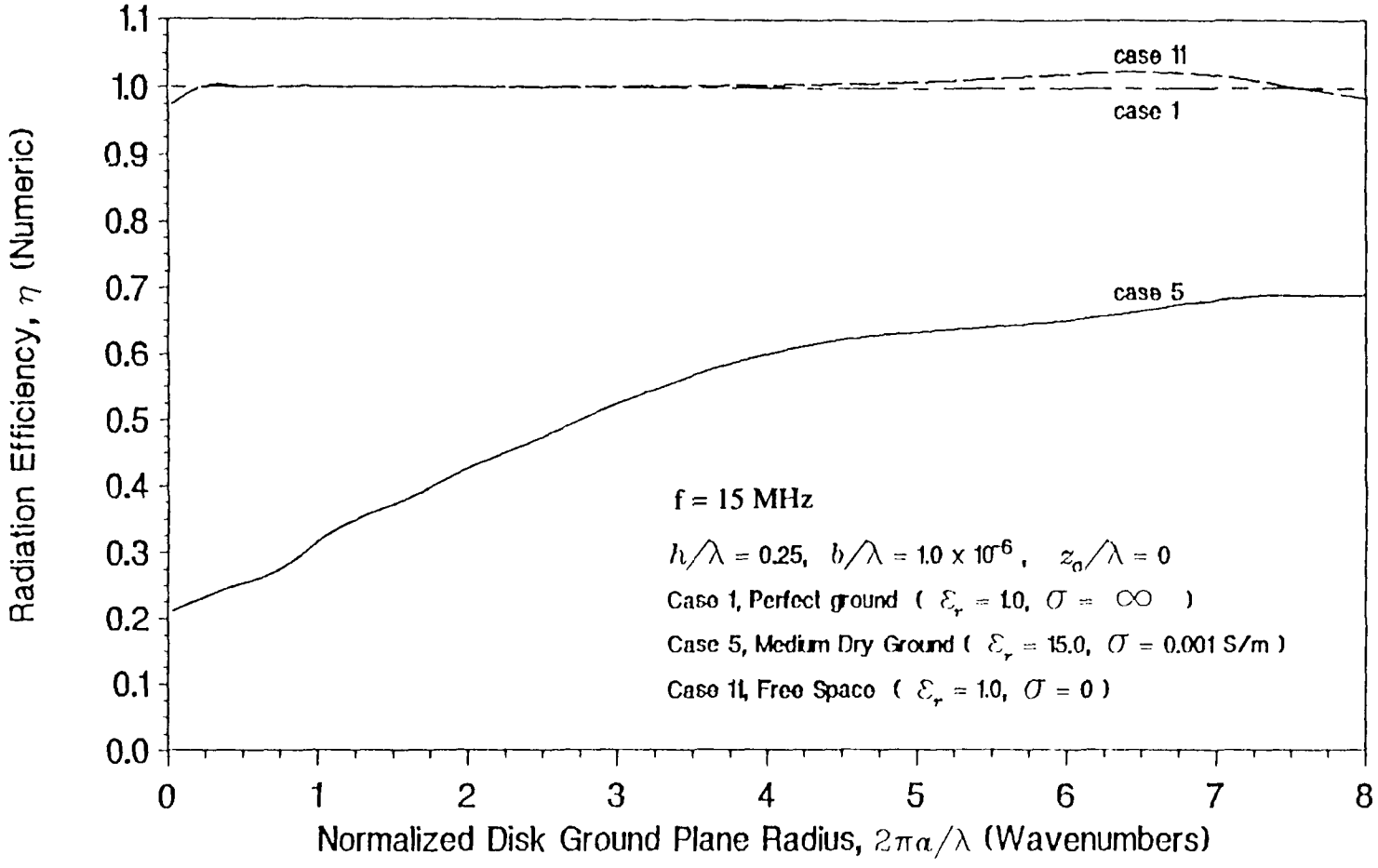

Figure 3-4. Radiation Efficiency of a Quarter-Wave Element on a Disk Ground Plane Resting on Medium Dry Ground

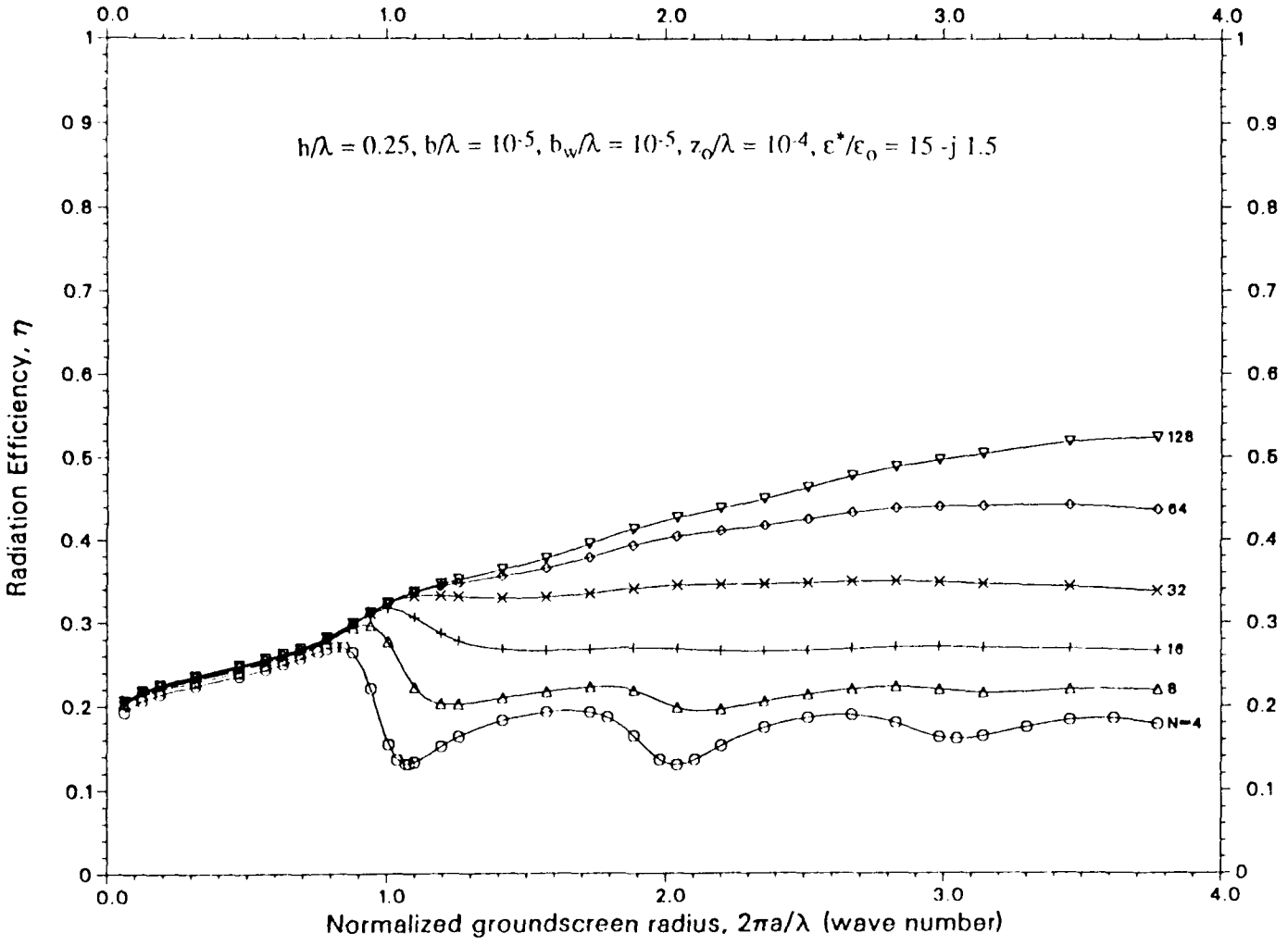

Figure 3-5. Radiation Efficiency of a Quarter-Wave Monopole Element on a Radial-Wire Groundscreen; $z_0/\lambda = 10^{-4}$, $\varepsilon^*/\varepsilon_0 = 15\text{-j } 1.5$

3.1.5 Role of Surface Wave in Directing Energy into the Earth

Why is the radiation efficiency (and modified reduction efficiency) of an electrically-short element in close proximity to Earth so small? If the source wavefront were a plane-wave incident at small grazing angles onto a semi-unbounded denser medium, most of the energy would be reflected. Instead, most of it is transmitted into the denser medium because a surface wave is generated.

In addition to energy being transmitted and absorbed into Earth by reflection of the direct and indirect waves, it is also directed into the Earth by a leaky evanescent surface wave that is generated in the air medium in proximity to the air-earth interface. The surface wave has an evanescent field in the air-medium only, but leaks energy into the Earth medium, not into the air medium [31]. The dipole radiation efficiency is small when the dipole is in close proximity to Earth because energy leaks into the Earth in the immediate vicinity of the dipole where the fields are strongest.

The explanation of the surface wave directing most of the available input energy into the Earth is consistent with the radiation pattern of figure 3-2. Most of the available input power is transmitted into the dielectric Earth at an angle of transmission equal to the critical angle. Goos and Hanchen [34] demonstrated the role of the surface wave in displacing the location of the reflected wave using a collimated narrow beam of light incident onto a less dense medium at angles of incidence greater than or equal to the critical angle.

The generation and analysis of surface waves are described in the literature extensively on the basis of the Sommerfeld integral (see list of references within reference 35). Booker and Clemmow [36, 37] determine the equivalent aperture distribution in the vertical plane that gives the surface and space-wave fields in the air medium above the Earth. The aperture distribution consists of the dipole, its image, and a line source extending indefinitely downward from the image. The line source, which generates the surface wave, disappears when the Earth is perfectly conducting. The aperture distribution yields an angular spectrum of reflected plane waves whose complex amplitude is determined by the Fresnel reflection coefficient for each angle of the spectrum. The

amplitude spectrum of the Fresnel coefficients is the Fourier transform of the aperture distribution. Brekhovskikh [38] combines the method of steepest descents (saddle points) with the decomposition of a spherical wavefront into an angular spectrum of plane waves to give a complete description of the direct wave, reflected wave, and surface wave at all points in space for a wide variety of cases, including the case of Goos-Hänchen. Brekhovskikh's analysis is applicable to spherical-wave refraction, whereas Fresnel's reflection and transmission coefficients are valid for plane-wave refraction by a semi-unbounded medium.

3.2 Ground-Plane Stabilization of the Available Loss Factors and Receiver Noise Factor

The available loss factors of the receive antenna, matching network, and transmission line (ℓ_c, ℓ_m, ℓ_n, respectively), and the receiver noise factor f_r are functions of the source impedance of each of the respective circuits. Consequently, these parameters are a function of the receive antenna input impedance which, in turn, is a function of the receive antenna ground-plane system.

3.2.1. Functional Dependence on Antenna Input Impedance

The impedance equivalent circuit of the receiving system is given in reference 28. Sequentially, the receiving system consists of the antenna, matching network, transmission line, and receiver. The receiving system available loss factors ℓ_c, ℓ_m, and ℓ_n of the antenna, matching network, and transmission line, respectively, are given by references 28 and 39 as:

$$\ell_c = R_{in} / R_{rad} = 1 + R_c / R_{rad} \tag{3-6}$$

$$\ell_m = 1 + [(R_m + R_s) / R_{in}] \tag{3-7}$$

$$\ell_n = \frac{\exp(2\alpha d)\{1 - |\Gamma|^2 \exp(-4\alpha d) - 2[\mathrm{Im}\, Z_o / \mathrm{Re}\, Z_o]\, \mathrm{Im}[\Gamma \exp(-2\gamma d)]\}}{1 - |\Gamma|^2 - 2\{\mathrm{Im}\, Z_o / \mathrm{Re}\, Z_o\}\, \mathrm{Im}\Gamma} \qquad (3\text{-}8)$$

where

R_{in} = antenna input resistance (ohms) = $R_{rad} + R_c$

R_{rad} = antenna radiation resistance (ohms)

R_c = series ohmic resistance of antenna circuit (ohms)

R_m, R_s = series resistances of matching network and its switching circuit, respectively (ohms)

Γ = voltage reflection coefficient looking back at the matching network = $(Z - Z_o) / (Z + Z_o)$

Z = output impedance of matching network (ohms) = $\begin{cases} Z_o, \text{ perfect matching network} \\ Z_{in}, \text{ no matching network} \end{cases}$

Z_o = characteristic impedance of transmission line (ohms)

Z_{in} = antenna input impedance = $R_{in} + j X_{in}$ (ohms)

α = attenuation coefficient of transmission line (m^{-1})

β = phase constant of transmission line (m^{-1})

d = length of transmission line (m)

= $\alpha + j\beta$ = propagation constant of transmission line (m^{-1})

Equations (3-6), (3-7), and (3-8) are functions of the antenna input impedance Z_{in}. In the absence of a matching network, $\ell_m = 1$. With a perfect matching network ($R_m = R_s = 0$, antenna is conjugate-matched to transmission line), $\ell_m = 1$ and $\ell_n = \exp(2\alpha d)$.

The receiver noise factor f_r is a function of the source admittance Y_{source} seen by the receiver looking back at the transmission line, given by reference 28 as

$$Y_{source} = \frac{1}{Z_o}\left[\frac{1 - \Gamma \exp(-2\gamma d)}{1 + \Gamma \exp(-2\gamma d)}\right] \qquad (3\text{-}9)$$

For a long lossy transmission line or a perfect matching network, $Y_{source} = 1/Z_o$. The receiver noise factor f_r is given by reference 28 as:

$$f_r = f_o + (r_n / \mathrm{Re}\, Y_{source}) |Y_{source} - y_{no}|^2 \qquad (3\text{-}10)$$

f_o = minimum noise factor of receiver for any possible source admittance Y_{source}

r_n = empirical receiver noise parameter with the dimensions of resistance that account for the sensitivity to source impedance of the receiver noise factor

y_{no} = $g_{no} + j\, b_{no}$ = complex empirical receiver noise parameter with the dimensions of admittance (Siemens)

Equations (3-9) and (3-10) are generally functions of the antenna input impedance Z_{in}.

3.2.2 Input Impedance of a Quarter-Wave Monopole Element on a Disk Ground Plane Resting on Earth

The antenna input resistance Z_{in} is given by

$$Z_{in} = R_{in} + j\, X_{in} = (R_{rad} + R_C) + j\, X_{in} \qquad (3\text{-}11)$$

where

R_{rad} = antenna radiation resistance (ohms) = $R_{in}\, \eta$

η = antenna radiation efficiency (numeric)

R_C = series ohms resistance of antenna (ohms) = $R_{in} - R_{rad} = R_{in}\,(1-\eta)$

Weiner [19] used Richmond's method-of-moments [20] to obtain the radiation resistance R_{rad}, input resistance R_{in}, and input reactance X_{in} of a quarter-wave monopole element on a disk ground plane resting on Earth for the CCIR-527-1 classifications of Earth given in table 2-1. Numerical results for medium dry ground at f = 15 MHz are presented in figures 3-6, 3-7, and 3-8. The radiation resistance R_{rad} increases periodically as the disk radius increases (see figure 3-6). The input resistance decreases aperiodically to an asymptotic value of 36 ohms as the disk radius increases (see figure 3-7). The input reactance increases aperiodically to an asymptotic value of 22 ohms for a very thin

monopole element (see figure 3-8). The input reactance is a stronger function of the element radius than the radiation resistance [40].

3.2.3 Input Impedance of a Quarter-Wave Monopole Element on a Radial-Wire Groundscreen in Proximity to Earth

Burke [33] has used his NEC-GS program to obtain numerical results of the input resistance R_{in} and input reactance X_{in} of a quarter-wave monopole element on a radial-wire groundscreen in proximity to Earth. These results are plotted in figures 3-9 and 3-10 for the groundscreen buried at a depth $z_o/\lambda = 10^{-4}$ in medium dry ground at f =15 MHz.

The input resistance and reactance asymptotically approach the radius for a disk ground plane as the groundscreen density approaches infinity (that is, as the number of radial wires $N \rightarrow \infty$). The resonances that occur in input impedance for a sparse number of radial wires (see figures 3-9 and 3-10) provided that the wires are not in proximity to earth of high conductivity [33], are a unique characteristic of radial-wire ground planes. They apparently occur because the currents on the sparse radial wires are not closely coupled, unlike those of the case for a high density of radial wires [33].

3.2.4 Antenna Input Impedance Stabilization with Respect to Ground-Plane Radius and Earth Permittivity

Antenna impedance mismatch is not as critical for receiving systems as it is for transmitting systems because the rf power levels in receiving systems are orders of magnitude less. Nevertheless, antenna impedance mismatch can cause a significant increase in the internal noise factor [28]. This problem is particularly acute in HF receiving systems because they usually employ electrically-short elements that must operate over a wide range of frequencies. Therefore, there is interest in stabilizing the antenna transmit mode input impedance so that the system remains externally noise-limited.

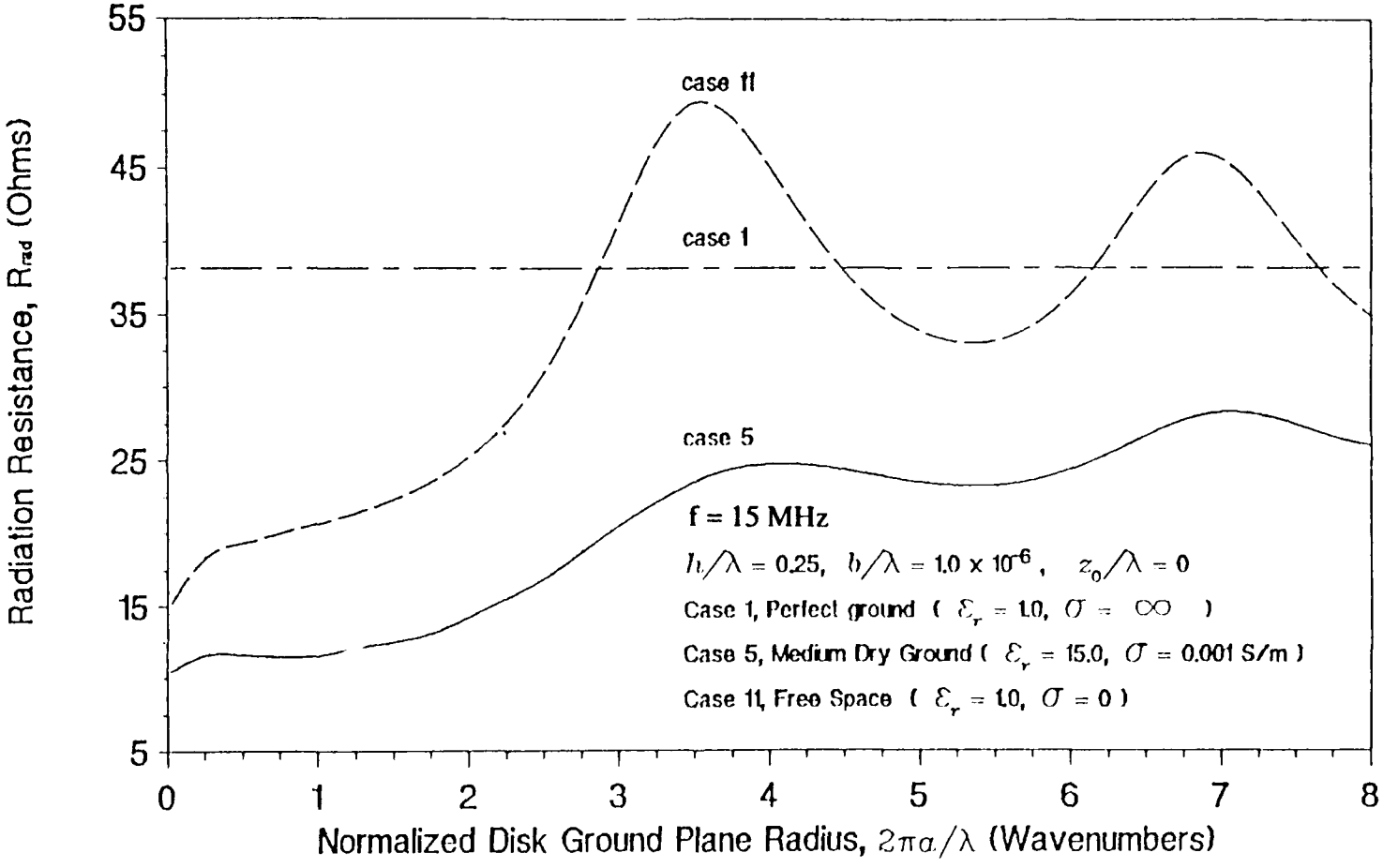

Figure 3-6. Radiation Resistance of a Quarter-Wave Monopole Element on a Disk Ground Plane Resting on Medium Dry Ground

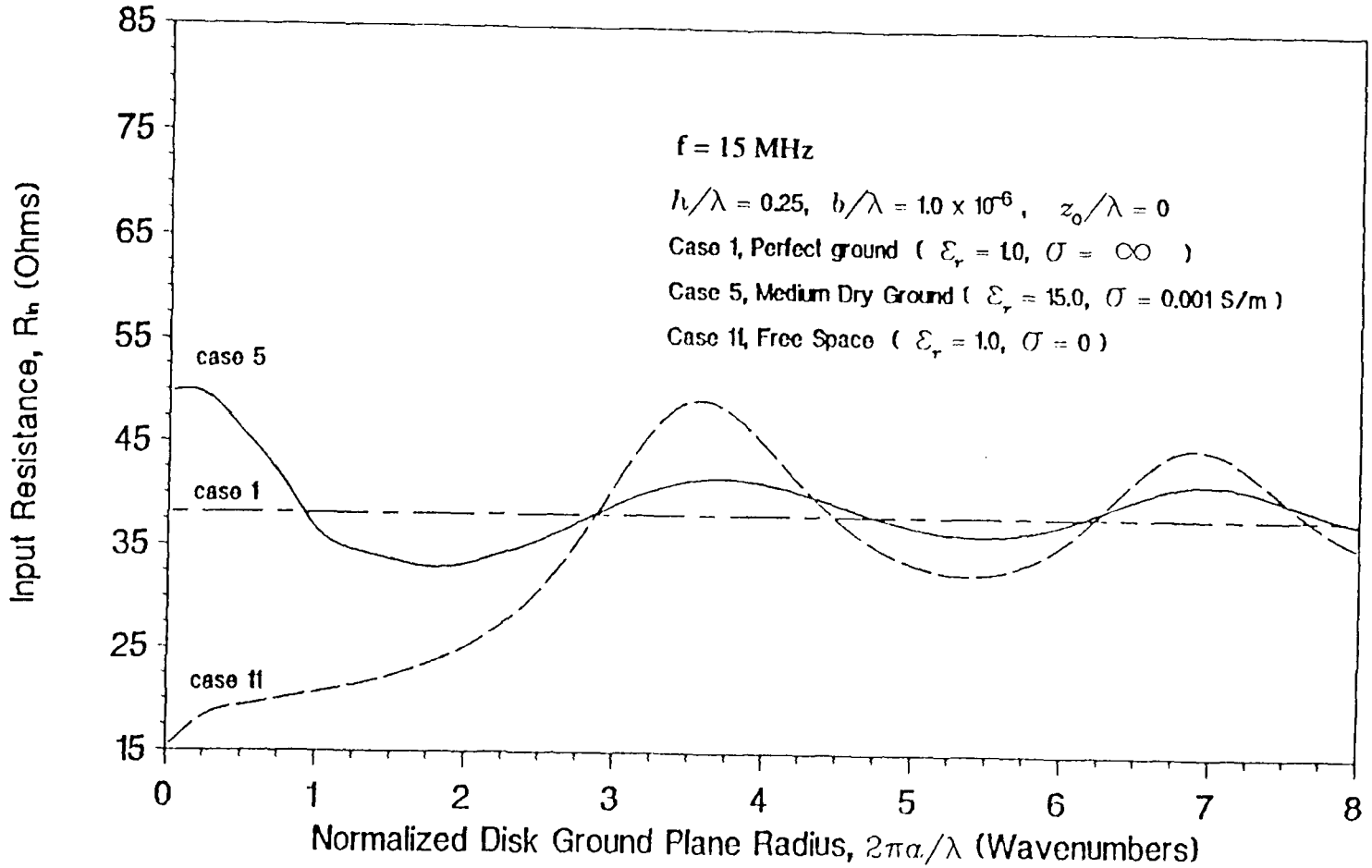

Figure 3-7. Input Resistance of a Quarter-Wave Monopole Element on a Disk Ground Plane Resting on Medium Dry Ground

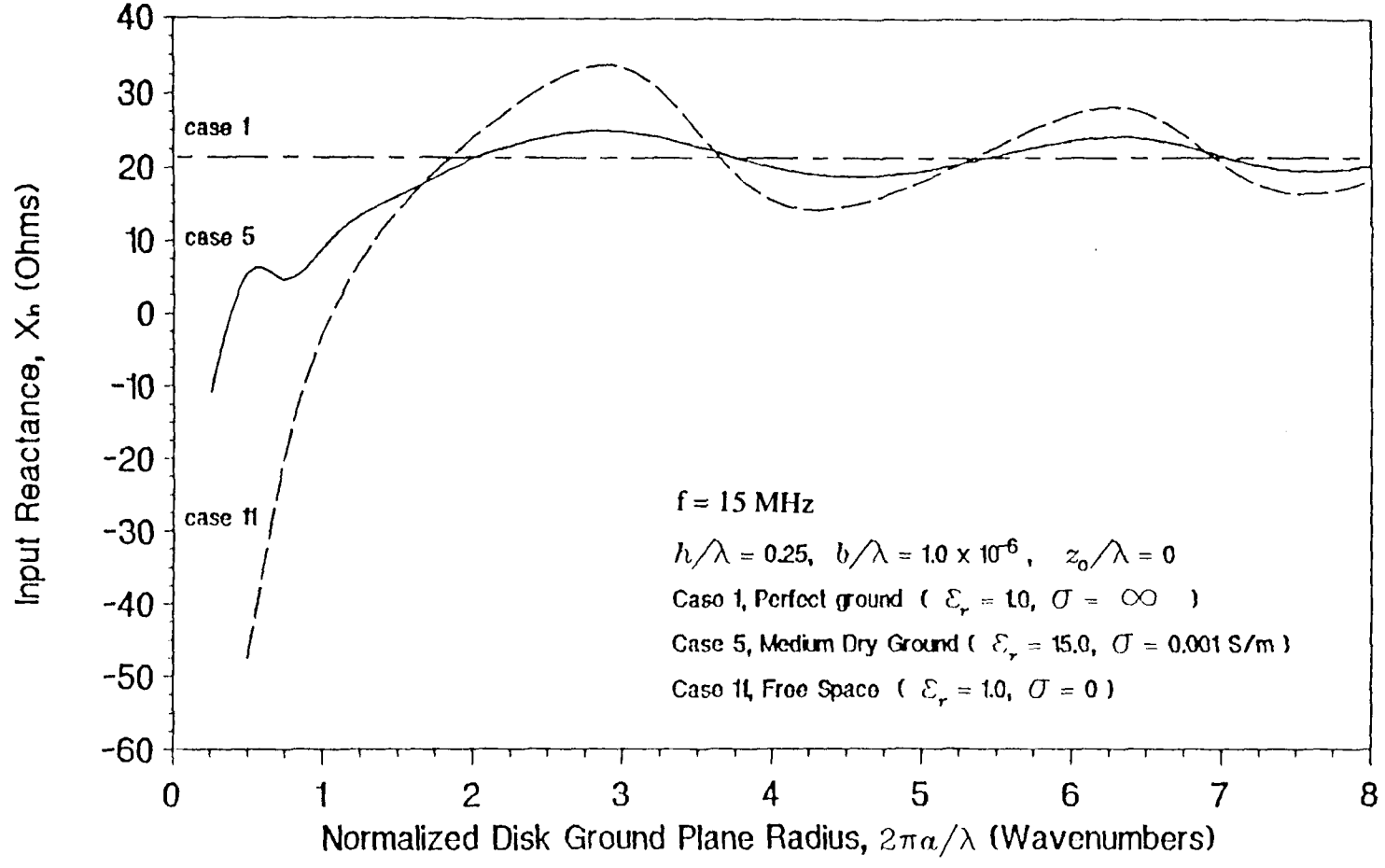

Figure 3-8. Input Reactance of a Quarter-Wave Monopole Element on a Disk Ground Plane Resting on Medium Dry Ground

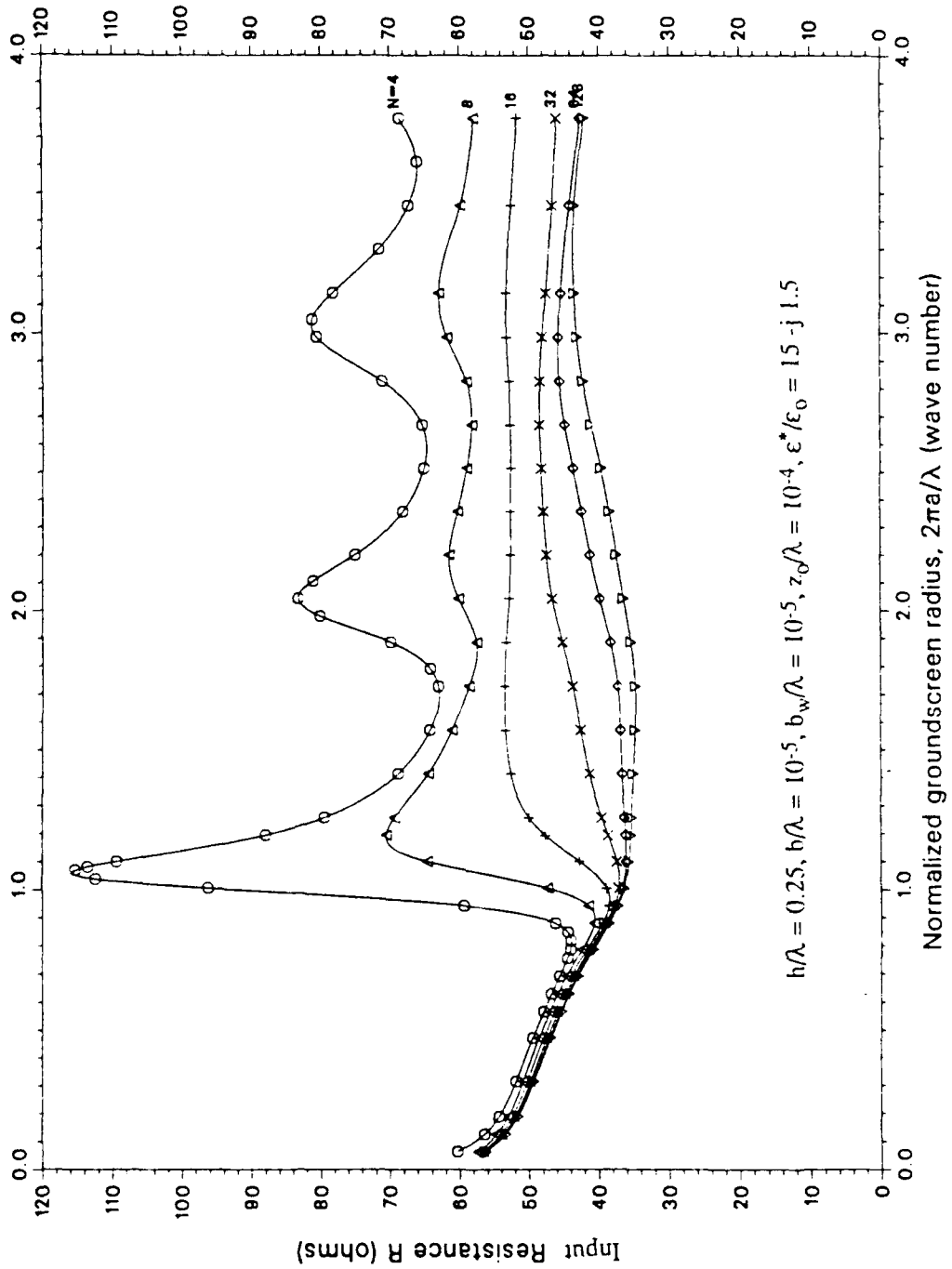

Figure 3-9. Input Resistance of a Quarter-Wave Monopole Element on a Radial-Wire Groundscreen; $z_o/\lambda = 10^{-4}$, $\varepsilon^*/\varepsilon_O = 15 - j\,1.5$

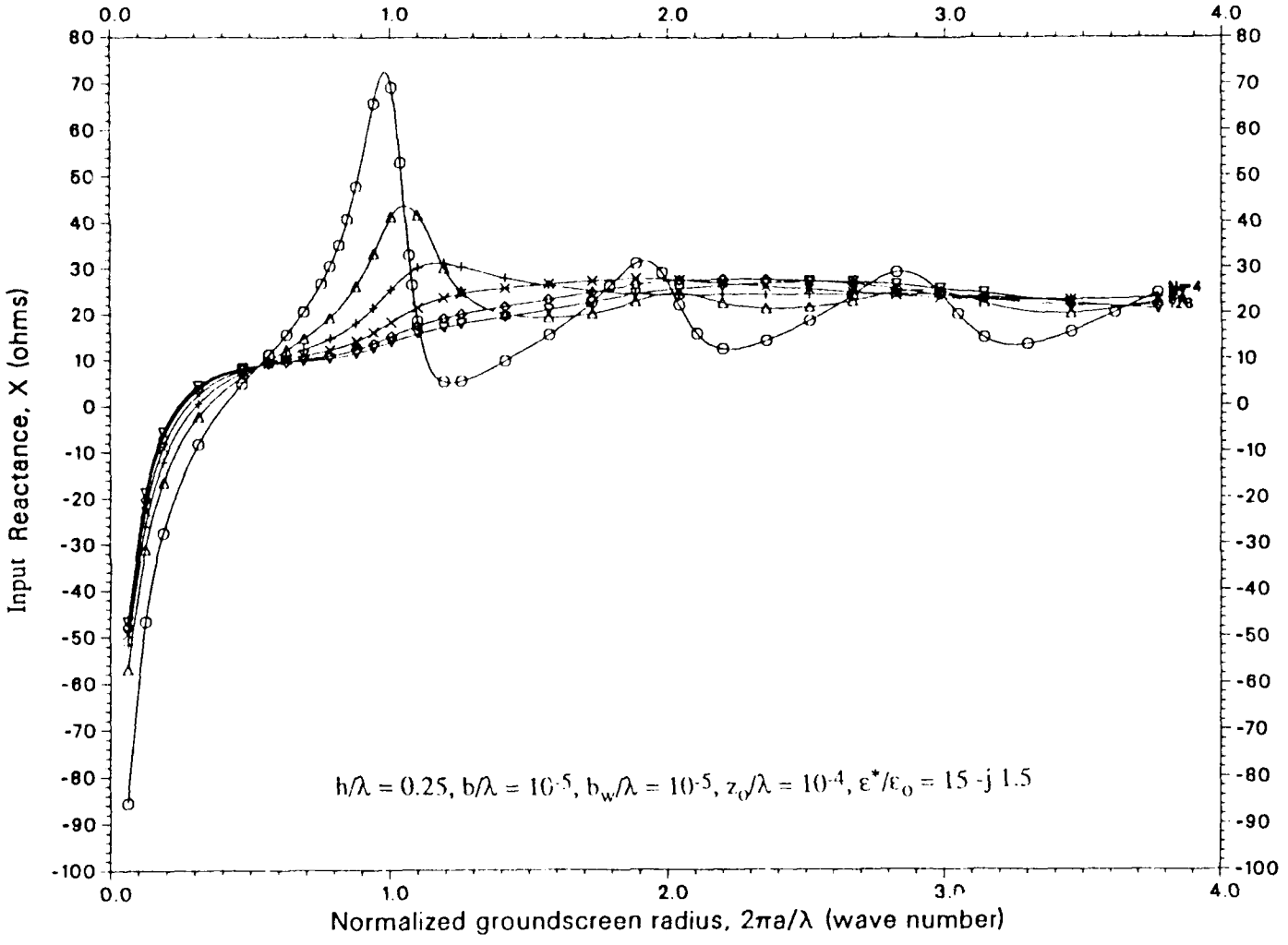

Figure 3-10. Input Reactance of a Quarter-Wave Monopole Element on a Radial-Wire Groundscreen; $z_0/\lambda = 10^{-4}$, $\varepsilon^*/\varepsilon_0 = 15 - j\ 1.5$

The antenna input impedance is a function of the normalized element length h/λ (the most influential parameter); the ground-plane system; and the normalized element radius b/λ which influences input reactance more than input resistance. The normalized ground-plane radius $2\pi a/\lambda$; groundscreen density (or number N of radial wires); normalized ground-plane height z_0/λ of the earth's surface relative to the ground plane; and Earth relative permittivity $\varepsilon^*/\varepsilon_0$ also affect input impedance.

Ground-plane radii of at least $2\pi a/\lambda = 2$ wavenumbers are required to stabilize the input impedance of quarter-wave elements with high-density ground planes to within 20 percent of that for a perfect ground plane (see figures 3-6 through 3-9). The minimum number of radial wires required to achieve this degree of stabilization is approximately N = 32 (see figures 3-8 and 3-9). The input impedance of monopole antennas with low-density ground planes is stabilized with ground-plane radii smaller than those required for high-density ground planes.

3.3 COMPARISON OF EXTERNAL NOISE FACTOR WITH CCIR PREDICTIONS

The external noise factor f_a in equations (3-1), (3-2), and (3-3) is a function of the directive gain (and, consequently, ground-plane characteristics) of the receive antenna unless the angular distribution $f(\theta,\phi)$ of the external noise is uniform in the hemisphere above lossy Earth. Within this section, we determine the external noise factor as a function of the ground-plane radius and compare the results with CCIR predicted values. For ground-plane radii less than at least eight wavenumbers, the external noise factor is approximately independent of the ground-plane radius and approximately equal to the CCIR predicted values in the HF band for the same angular distribution of CCIR external noise.

The external noise factor f_a of a receiving system is given in reference 1 as

$$f_a = (1/4\pi) \int_0^{2\pi} \int_{-\pi/2}^{\pi/2} f(\theta,\phi)\, d_r(\theta,\phi) \sin\theta \, d\theta \, d\phi \qquad (3\text{-}12)$$

where

$f_a(\theta,\phi)$ = external noise angular distribution (numeric with the same dimensionality as f_a and normalized to the same reference noise as f_a)

$d_r(\theta,\phi)$ = numeric directive gain of the receive antenna

For an antenna in proximity to lossy earth, $f(\theta,\phi) = 0$ and $d_r(\theta,\phi) = 0$ in the hemisphere below the ground. Therefore, equation (3-12) reduces to

$$f_a = (1/4\pi) \int_0^{2\pi} \int_0^{\pi/2} f(\theta,\phi)\, d_r(\theta,\phi) \sin\theta \, d\theta \, d\phi, \qquad \text{(3-13)}$$

antenna in proximity to lossy earth

For angular distributions of external noise that are either uniform [$f(\theta,\phi) = f_{ao}$] or a point source [$f(\theta,\phi) = (4\pi / \sin\theta_o)\, f_{ao}\, \delta(\theta - \theta_o)\, \delta(\phi - \phi_o)$], equation (3-13) reduces to

$$f_a = \begin{cases} f_{ao}, \text{ uniform angular distribution} \\ f_{ao}\, d_r(\theta_o, \phi_o), \text{ point source angular distribution for a source at } \theta=\theta_o,\ \phi=\phi_o \end{cases} \qquad \text{(3-14)}$$

for a source at $\theta = \theta_o, \phi = \phi_o$

The external noise factor is independent of directive gain for uniform external noise, but it is proportional to directive gain for a point source of external noise.

Section 2 demonstrates that the directive gain of a monopole element with a circular ground plane resting on lossy Earth is approximately independent of the ground-plane radius for ground-plane radii $0 \le 2\pi a/\lambda \le 8.0$ wavenumbers (see figures 2-2 through 2-13). Therefore, the external noise factor f_a is approximately independent of ground-plane radius for ground-plane radii at least as small as eight wavenumbers.

The CCIR (French) published statistical values of f_a for atmospheric noise in the frequency range 0.01 through 20 MHz based on measurements as a function of location, time of day, and season [41, 42]; and man-made noise in the frequency range 0.25 through 250 MHz based on measurements as a function of type of location [43]. These values, denoted by $f_{a\,CCIR}$, are claimed to be normalized to correspond to those values that would be measured with an electrically-short vertically-polarized monopole element mounted on a perfect ground plane [44, 45, 46]. It should be noted, however, that the antenna used for the CCIR measurements is a monopole element 21.75 feet long and a ground plane consisting of 90 radial wires (each 100 feet long and situated eight feet above the ground) [47]. The HF CCIR values most likely correspond to those values that would be measured with an electrically-short vertically-polarized monopole element mounted on an electrically-small ground plane in proximity to lossy Earth, as discussed in the remainder of this subsection.

The CCIR external noise factor f_{CCIR} is given by

$$f_{a\,CCIR} = (1/4\pi) \int_{o}^{2\pi} \int_{o}^{\pi/2} f_{CCIR}(\theta,\phi)\, d_{r\,CCIR}(\theta) \sin\theta \, d\theta \, d\phi \qquad (3\text{-}15)$$

where

$f_{CCIR}(\theta,\phi)$ = angular distribution of external noise for CCIR database

$d_{r\,CCIR}(\theta)$ = numeric direction gain of antenna for CCIR database

A receiving system's external noise factor f_a expressed in terms of CCIR external noise factor $f_{a\,CCIR}$ is found from equations (3-13) and (3-15) to be

$$f_a / f_{a\,CCIR} = \frac{\int_{o}^{2\pi} \int_{o}^{\pi/2} f(\theta,\phi)\, d_r(\theta,\phi) \sin\theta \; d\theta \; d\phi}{\int_{o}^{2\pi} \int_{o}^{\pi/2} f_{CCIR}(\theta,\phi)\, d_{r\,CCIR}(\theta,\phi) \sin\theta \; d\theta \; d\phi} \qquad (3\text{-}16)$$

Consider a receive antenna consisting of an electrically-short monopole element with an electrically-small ground plane resting on flat lossy Earth. Its directive gain $d_r(\theta, \phi) = d_r(\theta)$ is analytically approximated by equation (2-3) for and medium dry Earth and $2\pi a/\lambda = 3$ and is approximately valid for cases (3) through (11) of table 2-1 and ground-plane radii $0 \le 2\pi a/\lambda \le 8$ wavenumber. What is the ratio $f_a / f_{a\ CCIR}$ for the condition $f(\theta, \phi) = f_{CCIR}(\theta, \phi)$?

Since $f_{CCIR}(\theta,\phi)$ is unknown (the electrically-short monopole element used to obtain the CCIR database of $f_{CCIR}(\theta,\phi)$ is omnidirectional in the azimuthal direction and has poor angular resolution in the vertical plane), consider these arbitrary cases:

Case 1. $f_{CCIR}(\theta,\phi) / f_{a\,CCIR} = 1$

Case 2. $f_{CCIR}(\theta,\phi) / f_{a\,CCIR} = b \sin^8\theta$ where $b = 2 / [\int_o^{\pi/2} \sin^9\theta\, d_{r\,CCIR}(\theta)\, d\theta]$

Case 3. $f_{CCIR}(\theta,\phi) / f_{a\,CCIR} = b \cos\theta \sin^3\theta$ where $b = 2 / [\int_o^{\pi/2} \cos\theta\ \sin^4\theta\, d_{r\,CCIR}(\theta)\, d\theta]$

Case 1 corresponds to a uniform angular distribution. Case 2 corresponds to an angular distribution with a maximum gain on the horizon and a 50 percent value at $\theta = 66$ degrees. Case 3 corresponds to an angular distribution with a maximum gain at $\theta = 60$ degrees and a shape identical to that of $d_r(\theta)$ given by equation (2-3) for medium dry Earth and $2\pi a/\lambda = 3.0$.

If the values of $f_{a\,CCIR}$ have been normalized to correspond to those values that would be measured with an electrically-short monopole element on a perfect ground plane, then

$$d_{r\,CCIR}(\theta) = \begin{cases} 3\sin^2\theta, & 0 \le \theta \le \pi/2 \text{ rad} \\ & \text{, perfect ground plane} \\ 0, & -\pi/2 \le \theta < 0 \text{ rad} \end{cases} \qquad (3\text{-}17)$$

However, we contend that the values of $f_{a\,CCIR}$ in the HF band correspond more closely to those values that would be measured with an electrically-small ground plane. The ground-plane radial wires used to obtain the CCIR database are of length a = 100 ft. corresponding to $2\pi a/\lambda = 1.9$ and 19 wavenumbers at 3 and 30 MHz, respectively. In section 2, we showed that the directive gain pattern of monopole elements with ground planes resting on lossy Earth is not appreciably different for ground-plane radii $0 \le 2\pi a/\lambda \le 8$ wavenumbers. We suspect that the directive gain pattern for $2\pi a/\lambda \le 19$ wavenumbers more closely resembles that for an electrically-small ground plane than for an electrically-large ground plane. Except for normalization to correct for ohmic losses of the antenna system, it is doubtful that the CCIR values of $f_{a\,CCIR}$ are normalized to correspond to those for a perfect ground plane. That kind of normalization would require a knowledge of the elevation angular distribution $f_{CCIR}(\theta)$, which was experimentally not known; and the directive gain of monopole elements with electrically-small ground planes resting on lossy Earth, which was not known theoretically for disk ground planes until 1990 [19] and for radial-wire ground planes until 1989 [27]. Although the antenna input impedance for the radial-wire ground plane used to obtain the CCIR database is not appreciably different from that for a perfect ground plane, the directive gain pattern in the HF band at angles near the horizon is significantly different. Therefore, we contend that the numeric directive gain $d_{r\,CCIR}(\theta)$ of the antenna used to obtain the CCIR database could not have been normalized to that for a perfect ground plane. We further contend that the CCIR database in the HF band is better approximated by that for an electrically-small ground plane for ground-plane radii $0 \le 2\pi a/\lambda \le 8.0$ wavenumbers and possibly larger radii. Accordingly, $d_{r\,CCIR}(\theta)$ is better approximated by equation (2-3) than by equation (3-17); namely,

$$d_{r\,CCIR}(\theta) = \begin{cases} 10 \cos\theta \sin^3\theta, \; 0 \le \theta \le \pi/2 \text{ rad} \\ \\ 0, \; -\pi/2 \le \theta < 0 \text{ rad} \end{cases} \qquad (3\text{-}18)$$

electrically-small ground planes on lossy earth,
$0 \le 2\pi a/\lambda \le 8.0$ wavenumbers

The external noise factor of electrically-short monopole elements with electrically-small ground planes resting on lossy Earth is equal to the CCIR measured values for the same angular distribution of external noise, assuming that the values are normalized to those for a similar antenna (see table 3-2). However, if the CCIR measured values were normalized to those for an electrically-short monopole element with a perfect ground plane (which we dispute), then the external noise factor would be unchanged for uniform external noise; reduced by a factor $f_a / f_{a\,CCIR} = 0.69 = -1.6$ dB for external noise with a peak on the horizon; and increased by a factor $f_a / f_{a\,CCIR} = 1.19 = 0.8$ dB for external noise with a peak at 30 degrees above the horizon (see table 3-2).

These results suggest that the CCIR measured values of the external noise factor $f_{a\,CCIR}$ are not appreciably affected by the extent of the ground plane that was assumed in normalizing the CCIR values, provided that the external noise was angularly-distributed over a large solid angle. If the external noise factor is from a point source near the horizon, then the external noise factor is significantly affected by whether the ground plane is electrically-small or perfect. If it is electrically-small, the numeric directive gain is approximately zero near the horizon; however, if it is perfect, then the directive gain is a maximum on the horizon [see case 4 of table 3-2 and equation (3-17)].

Similarly, the peak intensity of the angular distribution of external noise is not significantly affected by the extent of the ground plane for a given external noise factor and shape of the angular distribution, provided that the external noise is angularly-distributed over a large solid angle. For example, the peak intensity of the angular distribution for electrically-small ground planes relative to that for a perfect ground plane will be unchanged for uniform external noise; increased by a factor of $(2.6/1.805) = 1.44 = 1.6$ dB for external noise with a peak at 30 degrees above the horizon (see table 3-2). However, if the external noise is from a point source on the horizon, the amplitude of the delta function distribution will increase by a factor of infinity (see table 3-2).

IL2827

Table 3-2. Comparison of External Noise Factor with CCIR Measured Values, $f(\theta) = f_{CCIR}(\theta)$

Receive Antenna: Electrically-short monopole element with an electrically-small ground plane resting on lossy earth

$d_r(\theta) = 10 \cos\theta \sin^3\theta$; $0 \le \theta \le \pi/2$ rad, zero otherwise

CCIR Antenna (1): Electrically-short monopole element with a perfect ground plane

$d_{r\,CCIR}(\theta) = 3 \sin^2\theta$; $0 \le \theta \le \pi/2$ rad, zero otherwise

CCIR Antenna (2): Electrically-short monopole element with an electrically-small ground plane resting on lossy earth

$d_{r\,CCIR}(\theta) = 10 \cos\theta \sin^3\theta$; $0 \le \theta \le \pi/2$ rad, zero otherwise

Case		Angular Distribution of CCIR External Noise $f_{CCIR}(\theta)/f_{a\,CCIR}$		External Noise Factor $f_a/f_{a\,CCIR}$	
No.	CCIR Noise Distribution	CCIR Antenna (1)	CCIR Antenna (2)	CCIR Antenna (1)	CCIR Antenna (2)
1	Uniform	1.00	1.00	1.00	1.00
2	Peak on Horizon	$1.805 \sin^8\theta$	$2.6 \sin^8\theta$	0.69	1.00
3	Peak at $\theta = 60$ deg	$4.667 \cos\theta \sin^3\theta$	$3.9 \cos\theta \sin^3\theta$	1.19	1.00
4	Point Source on Horizon	$0.667\,\delta[\theta - (\pi/2)]$	$A\,\delta[\theta - (\pi/2)]$, $A = \infty$	0	1.00

SECTION 4

ARRAY FACTOR DEGRADATION BY NONHOMOGENEOUS EARTH

The electric field, at each element of a ground-based HF receiving array, is the sum of a direct field and an indirect (multipath) field. For elements with sufficiently-small ground planes, the indirect field is not reflected from the ground plane; instead, it is reflected from the Earth in proximity to that element. The indirect field, relative to the direct field, is the product of the earth Fresnel reflection coefficient and a pathlength phase delay that is proportional to the height of the element above the Earth. The Fresnel reflection coefficient model is valid for computing directive gain, but not the absolute power gain (see section 3.1.1). If the Earth beneath the array is nonhomogeneous, then the argument of the total electric field at each element (after allowance for the true phase advance of the direct field at each element) is not uniform from element-to-element. The non-uniform argument causes an array rms phase error and beam-pointing errors when the nonhomogenous earth is systematically-distributed.

The earth Fresnel reflection coefficients and the arguments of the total field for a vertically-polarized Hertzian dipole at height h above the earth are tabulated in reference 48 for CCIR 527-1 classifications of Earth, and $h/\lambda = 0$, 0.54, and 0.270. The normalized heights $h/\lambda = 0$, 0.54 and 0.270 correspond to the midpoints at 6 MHz and 30 MHz, respectively, of a 5.4 m-length vertical monopole. The rms phase errors and beam-pointing errors are modeled in reference 48 for arbitrary distributions of nonhomogeneous Earth.

Numerical results are summarized in tables 4-1, 4-2, and 4-3 for randomly-distributed and systematically-distributed Earth nonhomogeneities for cases where one-half of the array elements is located in proximity to one type of Earth, while the remaining half is located in proximity to a second type. Very dry ground/medium dry ground, medium dry ground/wet ground, and very dry ground/wet ground combinations of Earth types are considered. The beam-pointing errors for randomly-distributed Earth nonhomogeneities are not shown in tables 4-1, 4-2, and 4-3 because the beam-pointing errors are zero for this case.

IL2649

Table 4-1. Summary of rms Phase Errors, Randomly-Distributed Two-Level Nonhomogeneous Earth

(a) 6 MHz (λ_o = 50m)

Angle of Incidence, θ (deg)	RMS Phase Error, α_{RMS} (deg)					
	Very Dry Ground/ Medium Dry Ground		Medium Dry Ground/ Wet Ground		Very Dry Ground/ Wet Ground	
	$h/\lambda_o = 0$	$h/\lambda_o = 0.054$	$h/\lambda_o = 0$	$h/\lambda_o = 0.054$	$h/\lambda_o = 0$	$h/\lambda_o = 0.054$
60	0.4	2.8	1.7	2.9	2.1	5.6
64	0.5	2.8	1.9	3.0	2.3	5.6
70	0.6	2.9	2.3	3.3	2.9	6.2
74	0.9	3.0	2.6	3.7	3.4	6.7
80	1.0	4.0	3.5	4.6	4.6	8.5
85	1.3	3.7	5.1	9.6	6.4	9.6
90	0	0	0	0	0	0

(b) 30 MHz (λ_o = 10m)

Angle of Incidence, θ (deg)	RMS Phase Error, α_{RMS} (deg)					
	Very Dry Ground/ Medium Dry Ground		Medium Dry Ground/ Wet Ground		Very Dry Ground/ Wet Ground	
	$h/\lambda_o = 0$	$h/\lambda_o = 0.270$	$h/\lambda_o = 0$	$h/\lambda_o = 0.270$	$h/\lambda_o = 0$	$h/\lambda_o = 0.270$
60	0.1	9.5	0.1	4.1	0.6	13.6
64	0.1	9.3	0.8	3.8	0.7	13.2
70	0.1	3.3	1.0	9.5	0.9	12.7
74	0.1	6.0	1.1	6.5	1.0	12.4
80	0.2	8.3	1.0	4.1	1.3	12.4
85	1.3	8.2	0.4	9.6	1.8	17.8
90	0	0	0	0	0	0

IL2653

Table 4-2. Summary of rms Phase Errors, Two-Level Nonhomogeneous Earth, Systematically-Distributed with Each Half of Array over Different Earth

(a) 6 MHz (λ_o = 50m)

Angle of Incidence, 0 (deg)	RMS Phase Error, α_{RMS} (deg)					
	Very Dry Ground/ Medium Dry Ground		Medium Dry Ground/ Wet Ground		Very Dry Ground/ Wet Ground	
	$h/\lambda_o = 0$	$h/\lambda_o = 0.054$	$h/\lambda_o = 0$	$h/\lambda_o = 0.054$	$h/\lambda_o = 0$	$h/\lambda_o = 0.054$
60	0.3	2.6	0.9	1.7	1.0	4.8
64	0.5	2.6	1.2	1.7	1.1	4.2
70	0.6	2.7	1.2	1.5	1.5	3.4
74	0.9	2.8	1.3	1.8	1.7	3.0
80	0.9	3.7	1.7	2.2	2.3	2.9
85	1.1	3.5	2.6	8.0	3.1	2.8
90	0	0	0	0	0	0

(b) 30 MHz (λ_o = 10m)

Angle of Incidence, 0 (deg)	RMS Phase Error, α_{RMS} (deg)					
	Very Dry Ground/ Medium Dry Ground		Medium Dry Ground/ Wet Ground		Very Dry Ground/ Wet Ground	
	$h/\lambda_o = 0$	$h/\lambda_o = 0.270$	$h/\lambda_o = 0$	$h/\lambda_o = 0.270$	$h/\lambda_o = 0$	$h/\lambda_o = 0.270$
60	0.1	8.8	0.3	4.8	0.9	6.7
64	0.1	8.7	0.5	2.0	0.6	6.5
70	0.1	3.0	0.5	3.2	0.5	6.3
74	0.1	5.6	0.6	4.6	0.4	6.3
80	0.2	7.7	0.4	1.9	0.4	6.1
85	1.2	7.5	0	2.0	0.1	8.8
90	0	0	0	0	0	0

IL2654

Table 4-3. Summary of Elevation Beam-Pointing Errors, Two-Level Nonhomogeneous Earth, Systematically-Distributed with Each Half of Array over Different Earth, $\phi = 0$ Degrees

(a) 6 MHz (λ_o = 50m)

Angle of Incidence, θ (deg)	Elevation Beam Pointing Error, $B_\theta/(BW)_{\theta,3\ dB}$					
	Very Dry Ground/ Medium Dry Ground		Medium Dry Ground/ Wet Ground		Very Dry Ground/ Wet Ground	
	$h/\lambda_o = 0$	$h/\lambda_o = 0.054$	$h/\lambda_o = 0$	$h/\lambda_o = 0.054$	$h/\lambda_o = 0$	$h/\lambda_o = 0.054$
60	0.01	0.05	0.03	0.05	0.03	0.16
64	0.01	0.05	0.03	0.05	0.04	0.14
70	0.01	0.05	0.04	0.05	0.05	0.11
74	0.01	0.05	0.04	0.06	0.06	0.10
80	0.02	0.07	0.06	0.08	0.07	0.09
85	0.02	0.06	0.08	0.10	0.10	0.09
90	0	0	0	0	0	0

(b) 30 MHz (λ_o = 10m)

Angle of Incidence, θ (deg)	Elevation Beam Pointing Error, $B_\theta/(BW)_{\theta,3\ dB}$					
	Very Dry Ground/ Medium Dry Ground		Medium Dry Ground/ Wet Ground		Very Dry Ground/ Wet Ground	
	$h/\lambda_o = 0$	$h/\lambda_o = 0.270$	$h/\lambda_o = 0$	$h/\lambda_o = 0.270$	$h/\lambda_o = 0$	$h/\lambda_o = 0.270$
60	-0.001	0.16	0.001	0.07	0.00	-0.22
64	-0.001	0.15	0.01	0.06	0.01	-0.22
70	-0.002	0.05	0.02	0.02	0.01	0.21
74	-0.002	0.10	0.02	0.11	0.02	0.20
80	0.004	0.14	0.02	0.07	0.02	0.20
85	0.02	0.13	0.01	0.16	0.03	0.29
90	0	0	0	0	0	0

The rms phase error is an increasing monotonic function of h/λ (for modest values of h/λ), but generally a non-monotonic function of the angle of incidence θ.

The maximum expected values of the rms phase errors at the best diffraction focus of the array for the cases examined are 18 degrees and nine degrees for randomly-distributed and systematically-distributed nonhomogeneities, respectively. The rms phase error is less for systematically-distributed nonhomogeneities because the linear phase error caused by beam-pointing errors has been subtracted. The maximum expected values of the beam-pointing error (in elevation and in azimuth) are zero and 0.3 beamwidths for randomly-distributed and systematically-distributed nonhomogeneities, respectively. The maximum rms phase errors and beam-pointing errors occur for very dry ground/wet ground, $\theta = 85$ degrees, $h/\lambda = 0.270$.

The above numerical results suggest that the influence of nonhomogeneous earth is appreciable, but not significant, on the performance degradation of an HF receiving array with electrically-small ground planes.

SECTION 5

SUMMARY AND CONCLUSIONS

Ground-based HF receiving arrays often employ some form of a vertical monopole element with a ground plane that is made as large as is economically feasible to mitigate the effects of the Earth and feed-cable exterior current on system performance. In the design of very large ground-based HF receiving arrays comprising hundreds or thousands of elements, electrically-large metallic ground planes are prohibitively expensive to construct and maintain. Economically, electrically-small ground planes are a relatively low-cost solution to this problem, provided the system performance is not too adversely affected. The performance of HF receiving arrays with electrically-small ground planes is investigated herein.

Electrically-small ground planes do degrade the performance of ground-based HF receiving arrays by reducing element directive gain near the horizon, distorting the element azimuthal pattern, increasing the system internal noise factor, and increasing the array factor rms phase error and beam-pointing errors. These performance degradations, however, are not significant for most applications.

Earth multipath reduces the directive gain near the horizon. The peak directive gain is approximately the same as that for a perfect ground plane except that the peak directivity is approximately 30 degrees above the horizon instead of near the horizon. The directive gain pattern is unaffected by the size of the ground plane for ground-plane radii at least as large as $0 \leq 2\pi a/\lambda \leq 8$ wavenumbers. The numeric directive gain, of electrically-short monopole elements with electrically-small ground planes resting on lossy Earth, is given approximately by $d_r(\theta) = 10 \cos\theta \sin^3\theta$; $0 \leq \theta \leq 90$ degrees zero otherwise. At angles near the horizon and for ground-plane radii at least as large as eight wavenumbers, the directive gain is reduced from the peak directive gain by approximately 4 dB at $\theta = 82$ degrees, 5 dB at 84 degrees, 7 dB at 86 degrees, 12 dB at 88 degrees, and ∞ dB at 90 degrees.

The exterior current on the element feed cable distorts the element azimuthal pattern and modifies the phase center of the element.

The system internal noise factor is increased by increased ground losses and antenna impedance mismatch. Whenever the antenna proximity to earth is not mitigated (by an electrically-large ground plane), the element ground losses are increased because of the generation of a leaky evanescent surface wave that directs energy into the Earth, but not into the air medium. The radiation efficiency of a vertically-polarized Hertzian dipole resting on Earth is zero if the Earth is lossy, and is approximately ten percent if the Earth is a perfect dielectric. The radiation efficiency of monopole antennas increases monotonically with increasing radius and density of the ground planes, and increasing length of the monopole element; it increases quasi-monotonically with increasing height of the ground plane above the Earth.

Antenna impedance mismatch can cause a significant increase in the system internal noise factor, particularly in HF receiving systems, because such systems usually employ electrically-short elements that must operate over a wide range of frequencies. Ground-plane radii of at least $2\pi a/\lambda = 2$ wavenumbers are required to stabilize the input impedance of quarter-wave elements with a high-density ground plane to within 20 percent of that for a perfect ground plane. The input impedance for a low-density ground plane is stabilized by ground-plane radii smaller than those for a high-density ground plane. Impedance-matching networks are generally necessary to achieve impedance matching over a wide range of frequencies. The ohmic loss of the matching network should be minimized so that the reduction in internal noise factor achieved by reduced mismatch loss is not offset by an increase in internal noise factor caused by those ohmic losses.

The external noise factor of HF receiving systems with electrically-small ground planes is expected to be comparable to CCIR predicted values. Although CCIR claims that their predicted values have been normalized to those for an electrically-short monopole element on a perfect ground plane, the ground-plane radial wires used to obtain the database are of length a =100 ft., corresponding to $2\pi a/\lambda = 1.9$ and 19 wavenumbers at

3 MHz and 30 MHz, respectively. The ground-plane radii are too small to yield a directive gain pattern at HF wavelengths that is appreciably different from that of a vertically-polarized Hertzian dipole resting on lossy Earth. It is doubtful that the CCIR values of the external noise factor are normalized to correspond to those for a perfect ground plane. This kind of normalization would require a knowledge of the elevation angular distribution of external noise, which was not experimentally determinable; it would also require knowledge of the directive gain of monopole elements with electrically-small ground planes resting on lossy Earth, but that was not known theoretically until recently.

The electric field at each element of a ground-based HF receiving array is the sum of a direct field and an indirect (multipath) field. For elements with electrically-small ground planes in proximity to nonhomogeneous Earth, the indirect field causes an array rms phase error and beam-pointing errors when the Earth nonhomogeneities are systematically-distributed. The maximum expected values of rms phase error, at the best diffraction focus of the array for very dry/wet nonhomogeneous Earth, are eighteen degrees and nine degrees for randomly-distributed and systematically-distributed nonhomogeneities, respectively. The maximum expected value of the beam-pointing error is zero and 0.3 beamwidths for randomly-distributed and systematically-distributed non-homogeneities, respectively.

The most significant performance degradation is the reduced directive gain at angles near the horizon. For applications that require better directive gain at those angles, the ground plane must be made electrically-large.

LIST OF REFERENCES

1. Weiner, M. M., August 1990, "Noise Factor and Antenna Gains in the Signal/Noise Equation for Over-the-Horizon Radar," MTR-10989, The MITRE Corporation, Bedford, MA, National Technical Information Service AD-A231203. See also *IEEE Trans. on Aerospace and Electronic Systems,* Vol. AES-27, No. 6, November 1991, pp. 886-890.

2. Weiner, M. M., S. P. Cruze, C. C. Li, and W. J. Wilson, 1987, *Monopole Elements on Circular Ground Planes*, Norwood, MA: Artech House, pp. 12-17.

3. Wait, J. R., and W. A. Pope, 1954, "The Characterization of a Vertical Antenna with a Radial Conductor Ground System," *Applied Scientific Research*, Vol. 4, Sec. B, pp. 177-195 (The Hague).

4. Wait, J R., April 1956, "Effect of the Ground Screen on the Field Radiation from a Monopole," *IRE Trans. on Antennas and Propagation,* Vol. AP-4, No. 2, pp.179-181.

5. Wait, J. R., 1963, "The Theory of an Antenna over an Inhomogeneous Ground Plane," *Electromagnetic Wave Theory*, edited by E. C. Jordan, pp. 1079-1097, Pergamon Press, Oxford.

6. Wait, J. R., and L. C. V iters, April 1963, "Influence of a Sector Ground Screen on the Field of a Vertical Ant na," *U.S. National Bureau of Standards*, Monograph 60, pp. 1-11.

7. Wait, J. R., 1967, "Pattern of a Linear Antenna Erected over a Tapered Ground Screen," *Canadian Journal of Physics*, Vol. 45, pp. 3091-3101.

8. Wait, J. R., September 1967, "On the Theory of Radiation from a Raised Electric Dipole over an Inhomogeneous Ground Plane," *Radio Science*, Vol. 2 (new series), pp. 997-1004.

9. Wait, J. R., 30 October 1969, "Surface Wave Effects with Large Antenna Earth Screens," *Electronics Letters*, Vol. 5, No. 22, pp. 552-553.

10. Wait, J. R., and K. P. Spies, 2 October 1969, "Fields of Electric Dipoles on Radially Inhomogeneous Ground Surface," *Electronics Letters*, Vol. 5, No. 20, pp. 478, 479.

11. Wait, J. R., and K. P. Spies, January 1970, "Integral Equation Approach to the Radiation from a Vertical Antenna over an Inhomogeneous Ground Plane," Radio Science, Vol. 5, pp. 73-79.

12. Wait, J. R., and K. P. Spies, July 1970, "On the Radiation from a Vertical Dipole with an Inductive Wire-Grid Ground System," *IEEE Transactions on Antennas and Propagation*, Vol. AP-18, No. 4, pp. 558-560.

13. Hill, D. A., and J. R. Wait, January 1973, "Calculated Pattern of a Vertical Antenna with a Finite Radial-Wire Ground System, " *Radio Science*, Vol. 8, No. 1, pp. 81-86.

14. Hill, D. A., and J. R. Wait, March 1973, "Effect of Edge Reflections on the Performance of Antenna Ground Screens," *IEEE Transactions on Antennas and Propagation*, Vol. AP-21, No. 2, pp. 230, 231.

15. Wait, J. R., September/October 1980, "Low Angle Radiation of an Antenna over an Irregular Ground Plane," Atti della Foundazione Giorgio Ronchi, Vol. 35, pp. 576-583, (Florence, Italy).

16. Wait, J. R., September 1990, "Antenna Performance Influenced by the Finite Extent and Conductivity of Ground Planes: A Collection of Reprints by J. R. Wait, et al.," M90-79, The MITRE Corporation, Bedford, MA, National Technical Information Service, AD-A232132.

17. Wait, J. R., August 1990, "Low Angle Radiation from HF Antennas," Symposium on Antenna Technology and Applied Electromagnetics, Winnipeg.

18. Rafuse, R. P., and J. Ruze, December 1975, "Low Angle Radiation from Vertically Polarized Antennas over Radially Heterogeneous Flat Ground," *Radio Science*, Vol. 10, p. 1011-1018.

19. Weiner, M. M., December 1990, "Input Impedance and Gain of Monopole Elements with Disk Ground Planes on Flat Earth," M90-92, The MITRE Corporation, Bedford, MA, National Technical Information Service, AD-A234284. See also *Proceedings, Progress in Electromagnetics Research Symposium (PIERS 1991)*, Cambridge, MA, 1-5 July, 1991, p. 691.

20. Richmond, J. H., June 1985, "Monopole Antenna on Circular Disk over Flat Earth," *IEEE Transactions on Antennas and Propagation*, Vol. AP-33, No. 6, pp. 633-637.

21. Richmond, J. H., "Far-Zone Field of Monopole Antenna on Circular Disk over Flat Earth," submitted to *IEEE Transactions on Antennas and Propagation*.

22. Burke, G. J., and A. J. Poggio, January 1981, "Numerical Electromagnetics Code (NEC) - Method of Moments," Lawrence Livermore National Laboratory, UCID-18834.

23. Burke, G. J., and E. K. Miller, October 1984, "Modeling Antennas Near to and Penetrating a Lossy Interface," *IEEE Trans. Antennas and Propagation*, Vol. AP-32, pp. 1040-1049.

24. Burke, G. J., February 1986, "Modeling Monopoles on Radial-Wire Ground Screens," *Applied Computational Electromagnetics Newsletter*, Vol. 1, No. 1.

25. Burke, G. J., January 1988, "A Model for Insulated Wires in the Method of Moments Code (NEC), Lawrence Livermore National Laboratory, Report 21301.

26. Burke, G. J., 1989, "Validation of NEC for Antennas Near Ground," Lawrence Livermore National Laboratory, Report UCRL-101190, NTIS DE89-1-06502.

27. Burke, G. J., and E. K. Miller, June 26-30, 1989, " Numerical Modeling of Monopoles on Radial-Wire Ground Screens," *Proceedings, 1989 IEEE AP-S International Symposium*, San Jose, CA, Vol. 1, pp. 244-247.

28. Weiner, M. M., March 1988, "Noise Factor of Receiving System with Arbitrary Antenna Impedance Mismatch," *IEEE Trans. Aerospace and Electronic Systems*, Vol. AES-24, No. 2, pp. 133-140.

29. Weiner, M. M., February 1986, "Available Loss Factor, Noise Factor, and Efficiency of a Mismatched Transmission Line," ESD-TR-86-240, The MITRE Corporation, Bedford, MA, National Technical Information Service, AD-A167104.

30. Hansen, P. M., November 1972, "The Radiation Efficiency of a Dipole Antenna Located above an Imperfectly Conducting Ground," *IEEE Trans. Antennas and Propagation*, Vol. AP-20, No. 6, pp. 766-770.

31. King, R. W. P., 1991, "On the Radiation Efficiency and the Electromagnetic Field of a Vertical Electrical Dipole in the Air above a Dielectric or Conducting Half-Space," *Progress in Electromagnetics Research (Pier 4)*, 1991, New York; Elsevier, Chapter 1.

32. Private communication from G. J. Burke, June 19, 1990, Lawrence Livermore National Laboratory.

33. Private communication from G. J. Burke, January 7, 1991, Lawrence Livermore National Laboratory.

34. Goos, F., and H. Hanchen, 1947, *Ann Phys.*, Vol. 6, No. 1, p. 333. A simplified description in English is found in A. R. VonHippel, *Dielectric and Waves*, 1954: John Wiley and Sons, NY, pp. 53-55.

35. King. R. W. P., 1990, "Electromagnetic Field of a Vertical Dipole over an Imperfectly Conducting Half-Space," *Radio Science*, Vol. 25, pp. 149-160.

36. Booker, H. G., and P. C. Clemmow, 1950, "A Relation between the Sommerfeld Theory of Radio Propagation over a Flat Earth and the Theory of Diffraction at a Straight Edge," *Proc. IEEE*, Vol. 97, Pt. III, pp. 18-27.

37. Clemmow, P. C., 1966, *The Plane Wave Spectrum Representation of Electromagnetic Fields*, Pergamon Press, Oxford.

38. Brekhovskikh, L. M., 1960, *Waves in Layered Media*, Academic Press, NY, 1st edition, chapter 4. Also available in a revised 2nd edition, 1980.

39. Weiner, M. M., July 1985, "Effect of Antenna Impedance Mismatch on the Signal-to-Noise Ratio of a Radio Receiving System," ESD-TR-85-136 (The MITRE Corporation, Bedford, MA), National Technical Information Service, AD-A159070.

40. op. cit,. 2, pp. 32-33, 92-94.

41. CCIR (1963), "World Distribution and Characteristics of Atmospheric Radio Noise," Report 322, 10th Plenary Assembly, Geneva (1963), Int. Radio Consultative Committee, Int. Telecommunication Union, Geneva, Switzerland, 1964.

42. CCIR (1983), "Characteristics and Applications of Atmospheric Radio Noise Data," Report 322-2, 15th Plenary Assembly, Geneva (1982), Int. Radio Consultative Committee, Int. Telecommunication Union, Geneva, Switzerland, 1983.

43. CCIR (1986), *Recommendations and Reports of the CCIR, 1986, Vol. 6*, "Man-Made Radio Noise," Report 258-4, 16th Plenary Assembly, Dubrovnik (1986), Int. Radio Consultative Committee, Int. Telecommunication Union, Geneva, Switzerland, 1984.

44. op. cit; 41, p. 6.

45. op, cit; 42, p. 4.

46. op. cit; 43, figure 1 caption, p. 208.

47. Ahlbeck, W. H., W. Q. Crichlow, R. T. Disney, F. F. Fulton, Jr., and C. A. Samson, 3 January 1985, "Instruction Book for ARN-2 Radio Noise Recorder, Serial Nos. 1 to 10," Report 5545, National Bureau of Standards, U.S. Dept. of Commerce.

48. Weiner, M. M., May 1991, "Influenced of Non-Homogeneous Earth on the Perfonnance of High-Frequency Receiving Arrays with Electrically-Small Ground Planes," MTR-11169, The MITRE Corporation, Bedford, MA, National Technical Information Service, AD-234288.

49. Lagace, R. L., December 1991, "Performance of the Monopole Antenna Element for the 96 - Element Receiving Array of the High-Frequency, High-Resolution Experimental Site," MTR-11291, The MITRE Corporation, Bedford, MA.

50. Weiner, M. M., September 1991, "Radiation Efficiency and Input Impedance of Monopole Elements with Radial Wire Ground Planes in Proximity to Earth," M91-104, The MITRE Corporation, Bedford, MA, National Technical Information Service, AD-A244578.

51. Weiner, M. M., September 1991, "Validation of the Numerical Electromagnetic Code (NEC) for Antenna Wire Elements in Proximity to Earth," MTR-11278, The MITRE Corporation, Bedford, MA